HHS Public Access

Author manuscript

Neuroimage. Author manuscript; available in PMC 2019 July 01.

Published in final edited form as:

Neuroimage. 2018 July 01; 174: 364–379. doi:10.1016/j.neuroimage.2018.02.059.

Abstinence to chronic methamphetamine switches connectivity between striatal, hippocampal and sensorimotor regions and increases cerebral blood volume response

Ji-Kyung Choi[a], **Grewo Lim**[b], **Iris Y Chen**[a], and **Bruce G. Jenkins**[a]

[a]A.A. Martinos Center for Biomedical Imaging, Department of Radiology, Massachusetts General Hospital and Harvard Medical School, Boston MA 02129

[b]Department of Anesthesiology, Massachusetts General Hospital and Harvard Medical School, Boston MA 02129

Abstract

Methamphetamine (meth), and other psychostimulants such as cocaine, present a persistent problem for society with chronic users being highly prone to relapse. We show, in a chronic methamphetamine administration model, that discontinuation of drug for more than a week produces much larger changes in overall meth-induced brain connectivity and cerebral blood volume (CBV) response than changes that occur immediately following meth administration. Areas showing the largest changes were hippocampal, limbic striatum and sensorimotor cortical regions as well as brain stem areas including the pedunculopontine tegmentum (PPTg) and pontine nuclei – regions known to be important in mediating reinstatement of drug-taking after abstinence. These changes occur concomitantly with behavioral sensitization and appear to be mediated through increases in dopamine D1 and D3 and decreases in D2 receptor protein and mRNA expression. We further identify a novel region of dorsal caudate/putamen, with a low density of calbindin neurons, that has an opposite hemodynamic response to meth than the rest of the caudate/putamen and accumbens and shows very strong correlation with dorsal CA1 and CA3 hippocampus. This correlation switches following meth abstinence from CA1/CA3 to strong connections with ventral hippocampus (ventral subiculum) and nucleus accumbens. These data provide novel evidence for temporal alterations in brain connectivity where chronic meth can subvert hippocampal – striatal interactions from cognitive control regions to regions that mediate drug reinstatement. Our results also demonstrate that the signs and magnitudes of the induced CBV changes following challenge with meth or a D3-preferring agonist are a complementary read out of the relative changes that occur in D1, D2 and D3 receptors using protein or mRNA levels.

Corresponding: Bruce G. Jenkins, bgj@nmr.mgh.harvard.edu or, Ji-Kyung Choi, jchoi@nmr.mgh.harvard.edu Building 149, 13th Street, Martinos Center for Biomedical Imaging, Department of Radiology, Massachusetts General Hospital, Boston MA 02129.

Conflicts of Interest: Dr. Jenkins consulted for Sunovion Pharmaceuticals on unrelated topics during performance of some of this work. No other conflicts are declared.

Keywords

Dopamine; functional connectivity; MRI; methamphetamine; sensitization; receptor

1. Introduction

Methamphetamine is one of the most widely abused drugs in the world. Statistics from the Office of National Drug Control Policy estimate 10.4 million people in the US have tried the drug, and it represents ≈8% of all treatment admissions in the US (http://www.drugabuse.gov/publications/research-reports/methamphetamine-abuse-addiction). Methamphetamine is one of the drugs of abuse most prone to relapse. Methamphetamine addicts have long term (2-5 years) relapse rates that can approach 90% according to NIDA, and even within one year relapse rates with treatment can approach 60% (Brecht and Herbeck, 2014). These statistics are very similar in other countries (McKetin et al., 2012). A number of crucial questions remain about brain circuitry and receptors changes that account for such high relapse rates. Further, the brain circuitry sub-serving various aspects of the behavioral features associated with drug abuse and models of drug abuse is slowly starting to come in focus, but there are still many aspects of which circuits are associated with which behaviors that remain to be either validated or demonstrated (Kalivas and Volkow, 2005; Koob and Volkow, 2010). In this study we were interested in long term memories of drug behavior that can trigger craving and relapse and may be modulated by associations between striatal/mesocorticolimbic and hippocampal circuitry following abstinence from drug (Adinoff et al., 2015; Schmidt et al., 2005). Thus, we investigated what happens to this circuitry when the animals chronically exposed to methamphetamine are rendered abstinent and then challenged later at different time points with methamphetamine. We specifically wanted to test the hypothesis of whether changes that occur following abstinence are much more profound than those that occur immediately following chronic methamphetamine – which might be expected based upon the time-dependence of the phenomenon of sensitization and its relation to drug seeking behaviors following withdrawal (Heidbreder et al., 1996) (Pickens et al., 2011) (Steketee and Kalivas, 2011). Using the power of non-invasive imaging we also wished to determine if there were novel, hitherto undiscussed, brain regions that may be modulated by chronic administration and cessation of methamphetamine.

We further wished to investigate what happens to dopamine receptor sub-types after chronic exposure, and then withdrawal, of methamphetamine. Although psychostimulants have been intensively studied in both contingent and non-contingent models of intake, there is still some disagreement over what happens to dopamine receptors in periods of abstinence. Some studies find up-regulation of, for instance D1 receptor (D1R) function, while others find decreases or no change in D1 receptor binding. Many, but not all, studies have reported decreased function of dopamine D2R (both post-synaptic as well as auto-receptors) following chronic intake of psychostimulants, including methamphetamine. Of special interest with regards to relapse behavior after abstinence are the D3R. D3R have been implicated in mechanisms leading to cue induced reinstatement of prior drug-seeking behaviors, but not in the drug-seeking behavior itself (Heidbreder et al., 2005; Higley et al.,

2011). Thus, study of D3R circuitry after abstinence may be particularly revealing with regards to relapse, and we wished to test the hypothesis that D3R are strongly upregulated following abstinence from methamphetamine compared to time periods close to chronic administration – a fact that is controversial based upon the few papers examining this issue (one finding an immediate, persistent, increase in D3R (Le Foll et al., 2005) and one finding a delayed increase (Neisewander et al., 2004)).

Magnetic Resonance Imaging (MRI) and in particular functional MRI (fMRI) (reviewed in (Lu and Stein, 2014)) or pharmacologic MRI (phMRI) has the potential to examine many of these questions by looking at dynamic changes in whole brain circuitry associated with psychostimulant intake and subsequent abstinence. Not only can information be obtained about which circuitry is altered, but administration of selective dopaminergic compounds can provide information on alterations in dopamine receptor sub-type selective circuitry and function. The response to drugs such as cocaine and amphetamine is driven largely by increases in synaptic and extrasynaptic dopamine that is then transduced into increased cerebral blood flow (CBF), cerebral blood volume (CBV) or blood oxygenation level dependent (BOLD) signals through D1/D5 receptor agonism and into negative CBF, CBV or BOLD through D2/D3 receptor agonism (Chen et al., 2005; Chen et al., 1997; Choi et al., 2006; Jenkins, 2012; Mandeville et al., 2013). Therefore, this tool provides a means to examine receptor adaptations to chronic methamphetamine administration using a technique with novel properties to those, mostly invasive and/or post-mortem, techniques applied previously.

In this manuscript we demonstrate that there are strong interconnections between prefrontal, limbic, hippocampal and sensorimotor circuitry that are modulated following abstinence from methamphetamine measured using methamphetamine or D3 agonist challenge. We also discovered a region of the dorsal striatum that manifests connectivity to the hippocampus that is strongly modulated by methamphetamine abstinence.

2. Materials and Methods

2.1 Animals

Male Sprague-Dawley rats between 250-300g were used in the study. Animals were housed with 12 hours light and dark cycle and ad libitum access to food and water. Animals were acclimated to the housing facility for at least 2 days before commencing the study. Animals were randomized to saline (SAL) or methamphetamine-treatment (METH) groups. The study protocol is shown in Fig. 1. Rats were subject to conditioning with methamphetamine or saline for 6 days and tested for conditioning on day 7. Then the animals were imaged on either two or nine days following meth or saline treatment (and one or eight days after CPP testing) and were tested for locomotor sensitization on either days 2 or 9 after CPP. A subset of the animals were culled on days 1 or 2 or 8 or 9 following CPP for receptor and mRNA assays after the imaging. We refer to the groups as SAL*early* (SAL*ear*) and SAL*late* and METH*ear*, METH*late* with the early and late subscripts referring to early after methtreatment (2-3 days after last day of conditioning) or late after meth-treatment (9-10 days after last day of conditioning). Each of the four groups were studied with either a meth challenge or a D3-preferring agonist for a total of eight groups. An additional group of naïve

animals was studied using imaging only as a baseline measure of the response to methamphetamine. All animal numbers are referred to in the figures and tables, but there were between 7-8 animals per group. All studies were conducted with approval from the Subcommittee in Research Animal Care at MGH and were conformant with the National Institutes of Health guide for the care and use of Laboratory animals. In addition, we have followed the ARRIVE guidelines for the animal studies (Kilkenny et al., 2010). The entire protocol is outlined in Fig. 1.

2.2 Behavioral Studies

2.2.1 Conditioned Place Preference—The basic CPP protocol was derived from that of Milekic et al. (Milekic et al., 2006) and consisted of three phases: habituation (day 0), conditioning (day 1-6), testing (day 7). The CPP apparatus is a Plexiglas box (Med Associates, St. Albans, VT) with two side-chambers of equal size (20.3 × 15.9 × 21.3 cm) separated by a middle chamber with a sliding door on each side. One chamber has white walls, a grid floor and is lit during the conditioning while the other has black walls, a smooth floor, and is not lit during the conditioning. For habituation (day 0), each rat was placed in the middle chamber with the door open. The rat was allowed to freely explore the apparatus for 10 min. The time spent in the light or dark chamber was automatically recorded. During the conditioning phase (day 1-6), rats were randomly divided into two groups (SAL vs. METH treatment). In the morning the METH group received 1 mg/kg i.p meth injection and was placed in the light chamber while the SAL group received the same volume i.p. saline injection and were placed in the dark chamber for 30 min. They were then returned to their home cages. Six hours later, both the SAL and METH rats received 1 mg/kg saline injection were placed in the dark chamber (METH group) or the white chamber (SAL group) for 30 min. For the post-conditioning test, rats were placed in the middle chamber and allowed to freely explore both chambers for 10 min. The time spent in the white chamber versus the black chamber is recorded.

2.2.2 Locomotor Sensitization—After the animals had been through the place conditioning the animals were tested one day after imaging (i.e. at either 2 days or 9 days after CPP) for locomotor sensitization. In this case the saline group would have received one dose of meth during the meth challenge in the magnet while anesthetized. For locomotor testing the animals were placed into an MED associates (St. Albans, VT) acrylic box (17×17in) covered in red transparent tape and a covered top with 16×16 infrared motion detectors. The software analyzes both distance traveled as well as rearing and stereotypy counts. The animals were allowed to habituate for 30 min in the chamber and then were injected with 1 mg/kg i.p. METH and locomotion was determined for another 30 min. The room in which the testing was done had a constant white noise background. Data were analyzed for total beam breaks as the sum of stereotypy and ambulatory counts in one minute time bins. Then the data in the 30 min post-meth were subtracted from the prior 30 min test without meth (or saline) since there is a correlation between the number of beam breaks before and after meth. Finally, the last 15 min of the differences were summed to avoid the initial part of the curve where locomotion is induced by novelty.

2.3 Pharmacologic MRI

Animals were scanned in a 9.4T Bruker (Billerica, MA) scanner. Animals were scanned in a head frame with ear and tooth bars and were kept warm with a circulating water blanket. Animals were scanned under halothane anesthesia in a mixture of air with supplemental oxygen (1-1.2% halothane in 30% O2/70% air). Animals had injections in the magnet through the tail-vein, under halothane anesthesia, of either meth (1mg/kg i.v.; Sigma, St. Louis MO) or the D3 agonist 7-hydroxy-**N**,**N**-di-**n**-propyl-2-aminotetralin (7-OHDPAT; 0.2 mg/kg i.v.; Sigma, St. Louis MO). The imaging protocol was similar to those we have published previously (Chen et al., 2010; Chen et al.,2011; Choi et al., 2006; Choi et al., 2010). Briefly, we used a tail-vein i.v. injection of iron oxide contrast agent Feraheme (ferumoxytol, Amag, Lexington, MA), to sensitize the images to cerebral blood volume (the IRON technique, Increased Relaxivity for Optimized Neuroimaging; (Chen et al., 2001;Mandeville, 2012; Mandeville et al., 2004; Mandeville et al., 2001)). Images were collected using a conventional gradient echo sequence (TR/TE; 400/7.5ms) with each image being collected in 0.85 min. Spatial resolution was 0.22×0.22mm in plane (128×128 matrix with a FOV of 28mm) with a slice thickness of 0.6 mm. Images were collected to follow the entire meth induced time course from onset until return to baseline. Four baseline images were collected and then Feraheme was injected at 17mg/kg followed 30 min later by either the meth or 7-OHDPAT and images were collected until the return to baseline.

Due to the necessity of survival for behavioral studies after imaging the animals were freebreathing in the magnet. We therefore examined changes in end-tidal CO_2 to determine if there were any differences between the METH and SAL animals. In a subset of animals end tidal CO_2 measurements were made after administration of meth under anesthesia. There was a small but significant decrease in end tidal CO_2 after injection of meth in both groups that peaked between 10-20 min before returning to baseline due largely to an increase in respiratory rate however there was no difference between the groups (ΔCO_2 = -8.1±1.6 in SAL vs. -5.8±1.8 in the METH animals (p=0.37; t-test)). In spite of these small decreases in CO_2, the effect of the meth was to cause a large increase in CBV in most brain regions.

2.4 Data Analysis

MRI data were registered to a standard template derived from the Paxinos atlas (Paxinos and Watson, 2006) using the program jip (http://www.nmr.mgh.harvard.edu/~jbm/jip). The images are aligned to the template using the usual six affine transformations as well corrections for nonlinear distortions, although due to the short TE the latter corrections were minimal. The alignment uses a bilinear interpolation of the slice thickness from 0.6 to 0.5 mm. The images were then motion corrected using AFNI (Analysis of Functional NeuroImages, NIH). No other transformations of the data were performed including spatial filtering or smoothing, or artifact removal (the use of anesthetized animals in head frames minimizes artifacts). After motion correction, images were converted on a voxel by voxel basis to CBV changes by converting signal intensity changes to ΔR2* on a pixel by pixel basis and assuming a linear relationship between R2* relaxivity and blood volume as we have published previously (Chen et al., 2010; Chen et al., 2011; Choi et al., 2006; Choi et

al., 2010) ($S_{POST} = S_{PRE}e^{-rCBV@T_E = T_E^{IRON}}$; $fCBV = {}^{\Delta V}\!/_{V}^{MEAS}(t) = 100\frac{\Delta R_2^{*MEAS}(t)}{R_2^{*IRON}}$)

The fCBV was defined as a percent change from baseline (rCBV) and then averaged over the full width half maximum of the signal change.

Regions of interest for the fCBV analysis were mostly drawn according to the Paxinos atlas (Paxinos and Watson, 2006) for the cortical regions, basal ganglia and subiculum. In the case of the anterior dorsal CPu, a region that has a different response to meth than does the rest of the CPu we drew ROIs determined from the diFC and CBV maps. In addition, it should be pointed out that many of the borders between cortical or thalamic areas (e.g. sensorimotor cortex S2 and barrel field cortex (S1BF)) identified in the Paxinos atlas are identified with a dotted line and are only best guesses without strong histochemical data supporting the borders. Although our voxel sizes were small it was still difficult to identify borders between parts of the dentate gyrus and hippocampal fields CA1 and CA3. We have therefore called the molecular layer of CA1 as CA1, but with the understanding that it could include some of the inner-blade of the dentate gyrus. Likewise, what we identified as CA3 was the most lateral region of the hippocampus near CA1 and CA2 that was unambiguously identified as CA3 in the Paxinos atlas. Likewise, we averaged together cingulate 1 and cingulate 2 and referred to it as medial prefrontal cortex (mPFCx) as that is the most commonly used term in drug abuse literature. The phMRI analyses indicated a region of the anterior dorsal caudate-putamen that responded differently to meth challenge. We segregated this region based upon the data analysis of the SAL animals using the unique signature (from both GLM of the fCBV data or from the diFC data) of opposite response. This ROI was used for the fCBV analyses. As discussed below we did not use an ROI analysis for the diFC data.

Drug-induced functional connectivity or correlation (diFC) analysis using AFNI was carried out on the averaged CBV data set by correlating the entire CBV time series derived from challenge with methamphetamine (not including the pre-iron oxide contrast baseline images) in response to the meth or D3 agonist challenge in the data set each voxel with every other – i.e. not ROI seed-based. It should be noted that this differs from resting state fMRI studies (even though the math is the same) due to the inclusion of the large response to the drug which is a primary driver of the correlations observed (see (Friston, 2011; Schwarz et al., 2009; Schwarz et al., 2007) for discussion of the issues). Thus, the diFC could just as readily be called drug-induced functional correlation, thus keeping the acronym the same, although this caveat also applies to other fMRI studies too. Nonetheless, as will be shown, there are very specific circuits identified in the diFC analyses.

This analysis generates a very large series of images (over 40K) that are derived from the voxel by voxel correlations across the image. In order to then generate correlation maps, the individual maps associated with a given voxel were averaged for a fixed number of voxels (between 6-24 voxels) sampled symmetrically across the brain adjusted for the size of the ROI, derived from within the predefined ROIs from the atlas as described above using CBV data. We consistently found that use of “seed-based” regions in rodent brain is unsatisfactory due to the fact that small changes in which voxels are included in the seed can have a large effect on the diFC maps. In order to demonstrate this fact we show the effects of generating

maps based upon moving small numbers of voxels in the hippocampus or using a hippocampal ROI as a seed region (see supplementary Fig. S1). It is apparent that there are large differences in the maps. Even though the spatial resolution is sub-millimeter for the functional studies the resolution we used (0.22×0.22×0.6 mm) is equivalent to only about 3 mm^3 in a human.

Another problem in assigning maps to specific circuitry is that some ROIs, like that from the anterior dorsal CPu, don't appear in any atlas so these were drawn on the basis of the GLM fitting to the CBV time courses. We also performed a random effects like analysis by examining the correlations between the average CBV integrated over the FWHM of the CBV time course in each of the ROIs for each of the animals derived form the fCBV data as described above.

For presentation purposes all diFC data were corrected for a false discovery rate where q = 0.05 (Z= 1.96) using the AFNI 3dFDR function and the data are presented with those thresholds, however the statistical comparisons between groups for ANOVAs and classifiers were made using the fCBV data.

2.5 Molecular Studies

2.5.1 Western Blots—Animals were sacrificed by decapitation under pentobarbital anesthesia. Brain regions of interest were separately removed and homogenized in an SDS buffer (20mM Tris-HCl, pH 7.5, 150mM NaCl, 1mM EDTA, 1mM EGTA, 2.5mM Sodium pyrophosphate, 1mM β-Glycerophosphate, 1mM Sodium Orthovanadate, 0.01% Tirton-X100, 0.01% NP-40) containing a cocktail of proteinase inhibitors (Roche, Indiainapolis, IN). The tissue homogenates were centrifuged at 12,000 rpm × 10 min at 4 °C. Samples (50 μg) were separated on an SDS-PAGE gel (4%–15% gradient gel; Bio-Rad, Hercules,CA) and transferred to polyvinylidene difluoride (PVDF) membranes (Millipore, Billerica, MA). Membranes were blocked with 5% nonfat dried milk and incubated overnight (4°C) with one of the following primary antibodies: D1, rabbit polyclonal, 1:500, (Millipore, Billerica, MA); D2, rabbit polyclonal, 1:800, (Millipore, Billerica, MA); D3, rabbit polyclonal, 1:200, (Santa Cruz Biotechnology, Santa Cruz, CA). Membranes were then incubated for 1 hour at room temperature with an HRP-conjugated secondary antibody (1:5,000; Santa Cruz Biotechnology, Santa Cruz, CA.). Blots were visualized in ECL solution (Thermo Fisher Scientific, Ashville, NC) for 5 minutes and exposed to x-ray films (Kodak, Rochester, NY) for 1 to 10 minutes. Blots were again incubated in a stripping buffer (67.5 mM Tris, pH 6.8, 2% SDS, and 0.7% β-mercaptoethanol) for 30 minutes at 50°C and reprobed with an anti–β-actin antibody (1:12,000, mouse monoclonal; Abcam, Cambridge, MA) as loading control. Western blots were made in triplicate. The density of each specific band was measured with ImageJ 1.34 s software (NIH, Bethesda, MD) and normalized against β -actin loading control.

2.5.2 Real-time—*RT-PCR* - Total RNA was isolated using TRIzol reagent (Invitrogen, Carlsbad,CA). Two micrograms of total RNA was used to synthesize the first strand of cDNA using SuperScript III kit (Invitrogen) according to the manufacturer's protocol. cDNA was diluted by 10-fold, and 1 μl of the diluted cDNA was used in a 20-μl PCR vessel. Real-

time PCR was used to analyze the gene expression of D1, D2 and D3. β-actin RNA gene expression was also measured as a control. PCR was performed by fluorogenic 5′ nuclease assay–based TaqMan real-time RT-PCR by using the ABI PRISM 7500 Sequence Detection System (Applied biosystems, Foster City, CA). Amplification was performed using the following primers: D1-5′ - CAGTCCATGCCAAGAATTGCC -3′ (forward), 5′ - AATCGATGCAGAATGGCTGGG -3′ (reverse) (Genbank accession number M35077) (Zanassi, et al., Journal of Neuroscience Research 58:544–552 (1999)); D2-5′ - CCACCACGGCCTACATAGCA-3′ (forward), 5′ -AATCTTGGCGTGCCCATTCT-3′ (reverse) (Genbank accession number M36831) (Medhurst, AD. Et al., Journal of Neuroscience Methods 98 (2000) 9–20), D3- 5′ - AGC ATC TGC TCC ATC TCC AAC CC-3′ (forward), 5′ - GCA CCT TTC CTG AGC CTT GAG GA-3′ (reverse) and 5′ - TACAACCTCCTTGCACC3′ (forward) and 5′ -ACAATGCCGTGTTCAATGG-3′ (reverse) for β -actin. PCR conditions used to amplify these genes were 55°C for 2 min, 95°C for 10 min, 40 cycles of 95°C for 20 sec and 65°C for 45 sec.

2.6 Statistical Analyses

2.6.1 Behavioral Testing—Comparisons of CPP conditioning or locomotor sensitization (pre and post) were made using paired t-tests as well as the Brown-Forsythe test for homogeneity of variance to test the hypothesis that conditioning produces an increase in animal response range. Since the variance increased after CPP conditioning (for both the saline and meth-treated animals) we used a Welch's t-test for comparisons with unequal variances.

2.6.2 Western Blots and PCR—Western blots and PCR for measurements of relative changes in D1, D2 and D3 receptors and mRNA were made in two different experiments. Comparisons were made between SAL and METH*ear* animals using a one-way ANOVA of treatment (METH/SAL) for each receptor corrected using a sequential Bonferroni-Holm for multiple comparisons (for D1, D2, D3R). Comparisons of the groups using both the time points were made using a two-way ANOVA for time (early or late) and treatment (METH or SAL), again using a Bonferroni-Holm correction for multiple comparisons.

2.6.3 fCBV—Data were compared using a one-way ANOVA for comparisons between the groups METH*ear*, METH*late* and SAL, using a Tukey-HSD post-hoc for intergroup comparisons. fCBV data, as described above, was taken averaged over the FWHM of the CBV time courses. Corrections for multiple comparisons were made using a Bonferroni-Holm. Similar comparisons were made from the diFC analyses using the R-values determined from the analysis. Tests for normality of the distributions of Rvalues showed the values were normally distributed using the brain ROIs using a Shapiro-Wilk W or Anderson-Darling test for all three groups (SAL, METH*ear*, METH*late*).

2.6.4 Machine Learning Classifiers—We used machine learning classification schemes to assign the various groups based upon the region of interest analysis of the regional fCBV changes. This provides an alternative approach to discriminating between groups compared to standard statistical analysis. In order to reduce the number of feature variables to a number more meaningful given the limited number of animals per group (i.e. to avoid over-

fitting) the data were first subject to a number of different attribute selectors including a relief f algorithm (Kononenko et al., 1997) and correlation feature selection with a greedy stepwise algorithm (Hall et al., 2009), and information gain algorithm we also used a p-value cut-off derived from the ANOVA analyses. These pre-processing steps led to a consistent set of brain regions that were then permuted for input, in groups of four, for use in classifiers. We used classifiers including Euclidean distance measures, multilayer perceptron, linear discriminant analysis and K-means clustering. These data were analyzed using WEKA (Hall et al., 2009).

3. Results

3.1 Conditioned Place Preference (CPP)

We randomly assigned rats to SAL or METH groups receiving saline or 1 mg/kg meth for six days and tested for CPP on day seven. Then animals were imaged either two days or nine days after the last meth dose with either meth (1mg/kg) or 7-OH-DPAT (0.2mg/kg) (see methods). As expected, six days of treatment with meth led to an increase in CPP as shown in Fig. 2a. There was no significant difference between the four METH groups, and all the treatments were exactly the same (the imaging and open field data being collected after the CPP) so the data are plotted together in Fig. 2a. There was a very significant increase in CPP after the six days of conditioning ($p<10^{-11}$; unpaired t-test assuming unequal variances (Welch's t-test)); n=38 METH; n=38 saline). We also found, as has not been reported before, that there was a significant increase in the variance post-conditioning in both the SAL and METH animals as tested for using a Brown-Forsythe test for homogeneity of variances (SAL pre vs. post; $F^* = 10.08$; $p < 0.01$; METH pre vs. post; $F^* = 33.8$; $p < 0.001$).

3.2 Alterations in Locomotor Activity

We measured alterations between the SAL and METH animals at 2 days and 9 days after CPP. Total beam breaks were measured automatically before and after meth injections. The animals show a large increase over time in beam breaks following meth (Fig. 2b). There was an increase in the locomotor activity in the METH*late* animals at 9 days following the last dose of meth, compared to the SAL group ($p<0.01$) measured as the sum of the difference (post – pre meth) of last 15 min following meth. At two days after the last dose of meth there was no significant difference between the METH*ear* and SAL groups (Fig. 2c). Even though there were fewer animals in this group, a power analysis shows that it would take 45-55 animals (depending upon the standard deviation) to detect a difference in the means with 80% power at an α of 0.05. Therefore, these results show that there is an increase in locomotor sensitization between 2 and 9 days post meth. There was no relationship between the degree of CPP and the locomotor response to methamphetamine in the meth treated animals ($R=0.35$; $p>0.2$), suggesting there may be different neuronal circuitry that sub-serves these phenomena. This finding is in agreement with the MRI data in that the CPP and open-field locomotor responses correlate with the fCBV changes induced by meth in different brain regions.

3.3 Changes in Cerebral Blood Volume (CBV) in Response to a Methamphetamine Challenge

For comparative purposes an averaged map of significant changes in CBV in response to a 1mg/kg meth challenge in naïve rats is shown in Fig. 3a,b. Increases in CBV are seen across much of the brain, with some areas, like cerebellum, hypothalamus or the hippocampus (CA1, dentate gyrus), showing negative CBV changes. These data are similar to those we and others have published previously for other dopaminergic ligands such as amphetamine or cocaine(Chen et al., 2005; Chen et al., 1997; Chen et al., 2010; Chen et al., 2011; Choi et al., 2006; Lu et al., 2014; Schwarz et al., 2009). Cortical sensorimotor areas have a smaller FWHM than those seen in caudate/putamen and thalamus (Fig 3, c-e). Interestingly, the medial prefrontal (mPFCx) and infralimbic cortex (ILmCx) show prolonged time courses matching those in the CPu and thalamus rather than sensorimotor cortex (SMCx). What is also clear in the maps, and has not been reported before by either our group or others using indirect dopaminergic agonists such as cocaine, CFT, meth, amphetamine or methylphenidate is that there is a region in the anterior dorsal CPu (ADCPu) that shows a small decrease in CBV in response to meth challenge (Fig 3a,e). This area has some very interesting properties as we describe later.

We scanned a group of saline and METH-treated animals (METH*ear*) the day following CPP testing with a 1mg/kg meth challenge. Then we scanned another group of animals (SAL/METH) at nine days following the last meth dose (METH*late*). Because the SAL*ear* and SAL*late* animals had identical fCBV changes in all brain regions examined, we consolidated then into one groups for the comparisons to the METH*ear* and METH*late* groups. Images showing the alterations in CBV are in Fig. 4b. In general, the CBV changes observed between the METH*ear* and SAL animals were quite similar except in a few regions. There was an increase in the full width half-maximum (FWHM) of the CBV time courses in infralimbic (SAL = 25.4±0.8 min; METH*ear* = 30.3± 1.7; ANOVA, $F_{1,23} = 8.9$ $p<0.01$) and mPFCx (SAL = 23.9±1.2 min; METH*ear* = 28.5±1.7; $F_{1,23} = 4.9$ $p<0.05$) and an increase in fCBV amplitude in ILCx (SAL = 14.5±2.5%; METH*ear* = 20.8±2.2%; $F_{1,23} = 6.8$ $p<0.05$). Other changes were not significantly different between the two groups. In the METH*late* animals there were much more profound changes observed in the phMRI data compared to the SAL or METH*ear* group. At this time point there were increases in CBV amplitude and FWHM in numerous brain regions including both limbic regions as well as highly significant changes in sensorimotor cortex compared to the saline group or the METH*ear* group (Table 1; Fig. 4c).

For meth challenge the degree of conditioned place preference was correlated with the fCBV change in the medial prefrontal cortex – with or without including the saline-treated animals (see Supplementary Fig. 2). Since the saline treated animals show an increased preference for the black chamber this suggests that the meth-induced changes in MPFCx fCBV are related to conditioning – whether for meth or saline. For meth treatment there were only three brain regions that showed significant correlations with the degree of sensitization as measured by beam breaks after methamphetamine, they were the motor region (M1,M2; $R = 0.68$; $p<0.05$); retrosplenial cortex ($R = 0.59$; $p <0.05$) and thalamus ($R =- 0.56$; $p<0.05$).

3.4 Alterations in Drug-Induced Functional Connectivity (diFC) as a Function of Time

We examined the changes in drug-induced FC in saline-treated, METH*ear* and METH*late* animals. The maps of diFC in both the SAL and METH*ear* animals are similar, there was a trend to lower overall diFC in the METH*ear* group, and this was significant for a number of brain region correlations. The overall trend for lower diFC between the 8 brain regions identified as providing the most contrast (Figs. 4 and 5) and all the other brain regions was, comparing Z-scores significant in all 8 brain regions (with Z values ranging from). In contrast, after 9 days of abstinence, there were widespread increases in diFC in the METH*late* group compared to both the SAL group and the METH*ear* group (Fig. 5). These changes reflect alterations in limbic and sensorimotor connectivity. Two representative maps are shown in Fig. 5 representing connectivity from infralimbic cortex and CA1. The ILmCx demonstrates strong correlations with sensorimotor cortex, striatum and thalamus that are increased dramatically at nine days after the last meth dose. There is much greater connectivity in the METH*late* animals between ILmCx and regions such as the PPTg and the pontine nucleus (at the bottom of the images – refer to Fig. 4) than in the SAL or METH*ear* animals. The high spatial resolution and high contrast to noise maps we collected allowed for characterization of important brain regions such as the CA1 and the PPTg. The CA1 region shows strong connectivity with septal areas, hypothalamus, CA3 and the anterior dorsal CPu (ADCPu). A correlation matrix for a random-effects connectivity model (Fig. 5c) shows that there is increased diFC between numerous sensorimotor and limbic areas in the METH*late* animals.

Due to the lack of discussion in the literature of what we are calling the anterior dorsal CPu (ADCPu) we show this area in detail in Fig 6. It can be seen that there is strong connectivity in the SAL animals between the ADCPu and the septum as well as the CA1 and CA3 fields in the hippocampus (Fig. 6a). These connectivities are very much weakened in the METH*late* animals where the ADCPu now increases connectivity with the NAcSh as well as the subiculum (Fig. 6a,b). Another area that has been little discussed in addiction research is the pontine nucleus. This region shows greatly increased connectivity in the METH group with many brain regions, as does the PPTg (Fig. 5; Supplementary Fig. S3 and S4). Conversely, the diFC is decreased between the hypothalamus and the rest of the brain in the METH*late* animals compared to the SAL animals (Supplementary Fig. S5).

3.5 Classifiers based upon brain circuitry CBV changes

We used machine learning tools to select out the brain regions that contributed to classification between the groups (SAL, METH*ear*, METH*late*) based upon the fCBV meth challenge data. We first used feature selectors to reduce the dimensionality of the problem and avoid over-fitting. We tested four methods to select the features (brain regions) to be used for the classifiers. We used a supervised relief F-ranking filter, a correlation feature selector using two different algorithms (greedy step-wise or genetic)(Hall et al., 2009) an information gain algorithm and an ANOVA p value ranking where the cutoff was specified as the p value corrected for multiple comparisons. Out of the 26 brain regions included, eight regions accounted for 76% of the total power to characterize the group segregation. All four methods converged on a similar group of brain regions including the hippocampus CA1 (4/4), subiculum (4/4), mPFCx (4/4), NAc (4/4), pontine nucleus (3/4), S2 (3/4), S1BF (3/4),

and hypothalamus (2/4). The attribute weighting for the top eight brain regions are shown in Fig. 7. We then took these eight brain regions and permuted them in groups of 4 and used simple K-means clustering as well as linear discriminant analysis (Fig. 7b). All permutations yielded only two clusters, with the SAL and all the METH*ear* groups clustering together and the METH*late* group segregated into its own cluster. A number of permutations yielded the best classification which classified with 93% overall accuracy. The fCBV changes associated with these eight regions are shown in Fig. 4c. We performed a linear discriminant analysis (LDA), as well as support vector machines classification. We also compared the CBV data between the three groups using similarity percentage indices using Euclidean distances (Sokal, 1961). Shown in Fig. 7b are the LDA data indicating that the METH*ear* and SAL animals are close and far from the METH*late* group. Euclidean distances (Fig. 7c) are also shown in the form of a triangle again confirming the large difference of the METH*late* animals from the other groups. Confusion matrices using either LDA or a multi-layer perceptron or a logistic regression (all with hold-out analyses) with permutations of four selected brain regions (to avoid over-fitting) showed mixing between the between SAL and METH*ear* groups more so than the METH*late* group. An example of two confusion matrices from a Multi-layer perceptron and a k-means cluster with logistic regression are shown here:

a	b	c		<-- classified as
10	3	2	|	a = SAL
4	2	1	|	b = METH*ear*
1	0	6	|	c = METH*late*
13	0	2	|	a = SAL
6	0	1	|	b = METH*ear*
0	0	7	|	c = METH*late*

We also compared the distribution of r values derived from the diFC from the eight brain regions to the other brain regions as shown in Fig. 7c for the SAL, METH*ear* and METH*late* groups. It is clear that there is an overall decrease in diFC in the METH*ear* group and a large increase in the METH*late* group as well as a large qualitative change in the maps of the METH*late* group (see Figs. 5 and 6) compared to the METH*ear* or SAL groups.

3.6 Increased Response to D3 receptor agonist stimulation after methamphetamine

Prior studies have shown an increase in D3 receptor expression levels in nucleus accumbens following administration of dopaminergic psychostimulants with some studies suggesting increased D3R expression 1 day following a single dose of cocaine (Le Foll et al., 2005) while others find increases only after many days of abstinence increasing from 2 days to 32 days (Neisewander et al., 2004). Given that phMRI provides an alternative means of assessing the function (rather than mRNA expression levels or ligand binding of prior studies) we hypothesized that the response to the selective D3 agonist 7-OHDPAT would be increased at 9 days compared to the 2 day abstinent group. 7-OHDPAT leads to decreased CBV in both METH and SAL animals. We found that there was an increase at both 2 and 9 days with no significant effect of time (two way ANOVA for treatment and time showed $F= 8.32$, $p<0.01$ for treatment and no effect of time $p>0.2$ and no interaction). Overall the largest increase in response was in the NAc consistent with the high expression of D3R in that brain region (Table 2). Corrections for multiple comparisons using a Bonferroni-Holm

showed the critical p value being 0.006 whereas the p value was 0.01, thus the change in NAc was on the borderline of significance depending upon how one corrects for multiple comparisons.

For D3 R, the degree of conditioned place preference (Wpost-Wpre) positively correlated with the increased negative CBV in the nucleus accumbens, but not other brain regions (n=29; $p<0.05$; $R = 0.54$; see Supplementary Fig. S2). There was no correlation between the beam breaks and the NAc CBV ($R = 0.11$; $p>0.5$).

3.7 Alterations in Functional Connectivity in Response to D3 Agonist

We also performed diFC analysis of the response to 0.2 mg/kg of 7-OHDPAT (Fig. 8). D3 agonist challenge results in decreased CBV in most brain regions (Choi et al., 2010), unlike the mostly positive fCBV changes noted with meth. These data showed that there was increased diFC in numerous regions in the METH animals from the accumbens. The strongest diFC, in both the SAL and METH animals occurs in the mPFCx, ILCx, ADCPu, thalamus and subiculum. Increases in diFC from the accumbens in the METH group was largest in ADCPu (20%), CPu (17%), thalamus (16%), subiculum (14%), and retrosplenial/occipital cortex (14%).

3.8 Alterations in Dopamine Receptors and mRNA Expression Levels

We measured alterations in dopamine D1, D2 and D3 receptors using western blots and mRNA expression (Fig. 9). Data collected from METH*ear* animals showed large increases in D1 and D3 receptor protein and mRNA levels in all the brain regions (NAc, CPu, mPFCx and VTA) and decreases in D2 protein and mRNA levels except in mPFCx where there was an increase in D2R (Fig. 9a). For the METH*late* animals we dropped the VTA but measured S1 cortex in order to test the hypothesis that the locomotor sensitization would be reflected in changes in receptor levels in sensorimotor cortex. There were significant increases in D1 and D3R in all brain regions studied. Further, the increases in D1 were larger at day 9 than at day 2 except in the CPu. Using two-way ANOVAs (time and treatment) showed that for D1R there were significant effects of treatment on receptor expression for S1 cortex, NAc, CPu, and mPFCx ($F_{2,15} = 78.7$, 46.3, 74.6 and 27.8 respectively; all p values <0.001). Significant effects of time on NAc and CPu ($F_{2,15} = 19.9$ and 11.1; $p <0.01$) and significant interactions between time and treatment for S1, NAc and mPFCx ($F_{2,15} = 8.8$, 6.9 and 7.0 respectively; $p<0.05$). For D3R there were significant effects for treatment on S1, NAc and CPu ($F_{2,15} = 27.7$, 32.0, 55.1 respectively; $p <0.001$) and significant effects of time on S1 ($F_{2,15} = 27.7$; $p = 0.0009$), but this latter significance is driven by the large change in saline animals over time. Overall these results show changes in DARs that match the signs and trends of the changes of CBV with meth treatment and subsequent abstinence. Quantitative comparisons between the phMRI and the mRNA and protein levels are difficult since we only measured the relative levels of the latter two.

One thing is clear is that the largest increases in D1R in S1, NAc and MPFCx occur at the METH*late* time point compared to the METH*ear* time point consistent with what we observed with the increases of fCBV in these brain regions (as well as many others). We found across all the four brain regions shown in Fig. 9b that there was a significant

correlation between increases in D1 protein levels and increased fCBV ($R = 0.504$; $p < 0.05$; See Supplementary Fig. S2), however there was no significant correlation between D3-induced fCBV and D3R ($R = 0.35$; $p > 0.17$).

4. Discussion

The data collected here show that there are large changes in brain circuitry and receptors that occur more than a week after meth administration ended. Cessation of meth led to large increases in fCBV and diFC that were paralleled by very large changes in D1 receptor expression (Fig. 9). We discuss the most prominent findings below.

4.1 Changes in fCBV and diFC following abstinence and sensitization

Numerous drugs of abuse show a similar pattern that retaking the drug after prolonged abstinence leads to euphoria that can precipitate relapse (Blum et al., 2009). Therefore we were interested in studying the effects of abstinence on the response to meth. We previously showed that there was a huge increase in diFC following cocaine challenge in rats trained to self-administer (SA) cocaine after 28 days of abstinence (Chen et al., 2011). There have also been large changes noted following abstinence in cocaine self-administering rats using resting state fMRI (Lu et al., 2014) as opposed to the drug-induced functional connectivity we performed here and in our prior paper.

Although we previously examined a 28 day abstinent time point using cocaine SA (Chen et al., 2011), we did not examine changes in diFC at earlier time points. However, we have unpublished data taken in collaboration with Mandeville, Kornetsky and Kossofsky that 1 day following cocaine SA there was little change in the CBV maps between saline and cocaine-treated animals except for subtle increases in FWHM of the medial prefrontal cortex similar to what we observed here with meth. Taken together these data show that the large increase in fCBV or diFC following abstinence was not dependent on drug (cocaine or meth) and not dependent upon contingent vs. non-contingent drug administration (i.e. self-administration vs. CPP). It would thus appear that this is a general feature of the consequences of cessation of chronic psychostimulant intake and may have some commonalities with what happens during sensitization (Robinson and Berridge, 1993, 2008; Zapata et al., 2003) (Steketee and Kalivas, 2011). Prior studies have shown that there are little differences between the magnitude of the increases seen in DA release and locomotion following sensitization between contingent and non-contingent administration of cocaine (Zapata et al., 2003). The pattern that we observed, of significant increases in diFC between nucleus accumbens, subiculum, brain stem, thalamus and sensorimotor cortical brain regions suggests a relation to the locomotor sensitization known to occur in these models.

We examined this issue further by performing correlations between fCBV changes induced by meth in the animals and we found that for meth treatment there were only three brain regions that showed significant correlations with the degree of sensitization as measured by beam breaks after methamphetamine, they were the motor region (M1,M2; $R = 0.68$; $p<0.05$); retrosplenial cortex ($R = 0.59$; $p <0.05$) and thalamus ($R =- 0.56$; $p<0.05$). This thalamo-cortical circuitry is involved in both movements (M1/2), as well as in planning and integration of movements (retrosplenial cortex; (Cho and Sharp, 2001)). Therefore, this

suggests that other elements of the large signal changes induced by abstinence in other brain regions, such as subiculum and NAc are not simply reflecting locomotor sensitization, but other phenomena related to upregulation of dopamine sensitization and neuronal plasticity that may be of relevance to relapse and reinstatement.

We also note that the large increases in fCBV and diFC to and from the limbic regions and pons accords with its prominent role in the “emotional motor system” in that the medial pons receives afferents almost exclusively from limbic regions (Holstege, 1995). The other general feature observed with these data is that brain regions known to be important for reinstatement of drug-taking such as the subiculum and the PPTg (Schmidt et al., 2009), show dramatically increased diFC with infralimibic cortex, medial prefrontal cortex and nucleus accumbens, suggesting why relapse rates are so high with drugs like methamphetamine (Brecht and Herbeck, 2014; McKetin et al., 2012).

There is some discussion in the literature about the relevance of sensitization to the circuitry related to relapse and other addiction-relevant behaviors. A very detailed review examined this question and concluded that much of the circuitry subserving sensitization is similar to that subserving reinstatement including the MPFCx, NAc, VTA, amygdala and hippocampus. The main difference seems to be in that the hippocampus interacts directly with the NAc for reinstatement rather than indirectly through the VTA-NAc connection in sensitization (Steketee and Kalivas, 2011). Our data clearly show strong interactions between the hippocampus and accumbens that are modulated with abstinence going from a more D2/D3-like interaction (negative fCBV) to a more D1-like interaction (positive fCBV changes). Another paper examined a novel proposed treatment for methamphetamine relapse and showed that the same drug treatment protocol that blocked behavioral sensitization to meth in a chronic methamphetamine treatment model also blocked reinstatement of drug-seeking behavior in a self-administration model (Davidson et al., 2007). Unfortunately, the CPP model is not optimal for testing reinstatement or relapse to drug-taking behavior, and contingent, self-administration models are more appropriate for testing such behaviors. Nonetheless, our data show large abstinence-induced increases in response to a chronically administered psychostimulants in both our prior contingent self-administration model data as well as the non-contingent model data here, thus this large increase may reflect a propensity to relapse and this needs to be tested in future studies.

Although there are a large number of papers examining the issue of sensitization to psychostimulants in rodents (with an extensive review dating back to 1986 (Robinson and Becker, 1986)), there are not as many examining the time dependence of this phenomenon. Most papers show that there is a time dependent increase in locomotor sensitization to both cocaine and meth (Heidbreder et al., 1996; Henry and White, 1991; Robinson and Becker, 1986). While the magnitude of the changes can be dependent upon the timing and frequency of the treatment, one constant feature of all studies is that changes that occur are enduring. More recent studies indicate that this sensitization can be elicited by either D2 receptor down-regulation or D1R up-regulation i.e. the D1/D2 ratio (Thompson et al., 2010). Studies of D3 knockout mice show a decrease in locomotor sensitization suggesting that D3R are also involved behavioral sensitization (Zhu et al., 2012). In our data we observed both phenomenon (i.e. D2 downregulation and D1/D3 upregulation) which may lead to the large

effect sizes we noted for the changes in diFC as well as explaining the increases in fCBV in the METH*late* animals. These results suggest a dramatic alteration in brain circuitry that could have a profound effect on potential sensitivity to drug cues leading to relapse since humans, like rodents, also exhibit sensitization.

4.2 Alterations in connectivity between hippocampal, brain stem and mesocorticolimbic circuitry

We found profound changes in hippocampal regions and brain stem. Using machine learning, we found the regions that most strongly discriminate between groups were the CA1, subiculum, nucleus accumbens, mPFCx, SMCx and pontine nucleus. Strong increases in diFC between subiculum and nucleus accumbens were found after meth treatment. This provides support for an hypothesis put forward by Lisman and Grace suggesting that disinhibition of the nucleus accumbens neurons from the subiculum allows for the burst firing characteristic of reward (Lisman and Grace, 2005). The anterior cingulate and infralimbic cortices (which overlap considerably in the rat and are often referred to together as the medial prefrontal cortex mPFCx) have direct projections to the subiculum thus providing a means to interact. Our data provides evidence that this interaction is mediated through both D1 and D3 receptors as we found similar increases in fCBV and diFC in the accumbens and subiculum as a consequence of chronic meth using either a meth or D3 agonist challenge. Further, we previously showed that different D3 agonists as well as D3 antagonists strongly affect the subiculum – accumbens – medial prefrontal circuitry (Choi et al., 2010; Grundt et al., 2007). Importantly, increases in diFC noted in this study occurred with agents that lead to largely positive CBV changes (meth) or negative CBV changes (D3 agonist). In this regard, studies of the role of the subiculum show that inactivation of this region with focal lidocaine or GABA agonist injections in rats does not block lever presses for cocaine, but does block cue-induced reinstatement (Black et al., 2004; Lasseter et al., 2010; Rogers and See, 2007) similar to what has been discovered with D3R antagonism (Andreoli et al., 2003; Cervo et al., 2007; Gilbert, 2005; Higley et al., 2011) and its affects on reinstatement, but not reinforcement (Caine et al., 2012). A recent study showed that reinstatement of cocaine self-administration could be blocked by injection of D2/D3 antagonist but not D1/D5R antagonists in the subiculum (Keralapurath et al., 2014) highlighting the role of the D3 receptor in this process and anatomical disconnection of the subiculum – nucleus accumbens shell, but not subiculum-medial prefrontal cortex blocked cue-induced reinstatement of heroin seeking (Bossert et al., 2015). These results suggest that the subiculum – striatal circuitry plays an important role in memory of the drug exposure.

4.2 Anterior Dorsal Caudate-Putamen

We discovered that there was a region of the anterior dorsal CPu (including medial and lateral dorsal regions) that shows decreased CBV in response to meth compared to the rest of the CPu in both the naïve and SAL animals (Fig. 3,4,6). This area shows strong diFC with the molecular layer of the CA1 fields (molecular and/or stratum radiatum layers) of the hippocampus, hypothalamus, septum and ventral pallidum that was completely altered in the METH*late* animals, showing a change of connectivity to nucleus accumbens and subiculum instead of CA1, septum and hypothalamus (Fig 6b). We searched the literature for stains including D1, D2 and D3R, Nissl, tyrosine hydroxylase, GAD, ChAT and others and

compared these stains to the maps shown in Fig. 6. The only stain that had the same spatial pattern as the observed image is the stain for calbindin. To facilitate this comparison, we took a single slice from the MRI to compare to the calbindin stain from data published by Reidel et al. (Riedel et al., 2002). The comparison is shown in Fig. 6c. It is clear that the same regions manifesting negative fCBV (septum and ADCPu), are very lightly stained for calbindin, whereas areas manifesting positive CBV including accumbens and the lateral CPu show high staining for calbindin. Interestingly, the medial part of ADCPu was found to produce surges in enkephalin in rats eating chocolate (DiFeliceantonio et al., 2012). Enkephalin would be expected to decrease CBV through gabaergic mechanisms potentially explaining the decreased CBV seen in this region during meth stimulation. Activation was seen in cocaine cue-induced fMRI in "dorsolateral" striatum that differentiated cocaine from natural rewards (Liu et al., 2013) implicating the importance of this region for psychostimulant associations. *Future studies should, however, pay more attention to the location of probes and ROIs etc. when studying "dorsolateral striatum" as our data show that what we are calling ADCPu is more spatially circumscribed compared to what is typically considered dorsolateral striatum in rodents*.

4.3 Relation to prior studies of Functional Connectivity in humans drug abusers

A number of studies have appeared assessing alterations in functional connectivity in either cocaine or methamphetamine abusers. Most of these studies show decreased connectivity connecting dorsolateral prefrontal cortex to midbrain and increased connectivity in the mesolimbic circuitry in methamphetamine abusers (Kohno et al., 2014) (Konova et al., 2013) (Kohno et al., 2016) (London et al., 2015) that may bias psychostimulant users away from impulse inhibition and towards reward. Studies of cocaine abusers show similar findings and find decreased connectivity in executive and cognitive control circuitry (Ray et al., 2016) as well as deficits in attentional circuitry (Tomasi et al., 2010) and motor and visual circuitry (reviewed in (Lu and Stein, 2014)). Our finding of similar alterations of diFC that increased connectivity between, for instance, accumbens and ventral hippocampus (subiculum) but show decreased connectivity between dorsal hippocampus and mesocorticolimbic circuitry suggests that some of these observations may generalize across species. It is also of interest that we found decreased connectivity at the early time point (METH*ear*), but greatly increased connectivity following abstinence. However, to be fair, most of the human studies report changes in resting state or task-induced connectivity rather than the diFC reported here. The use of a methamphetamine or D3 agonist challenge drives the signal to, in our opinion, be more strongly weighted towards maps reflecting the connectivity of dopaminergic signaling than can be anticipated in resting-state studies.

4.4 Receptor Modulation: Changes in binding, protein levels or mRNA expression?

Changes in receptor levels are typically measured using receptor binding with selective ligands (as in PET or post mortem autoradiography), measuring protein content with specific antibodies (e.g. Western Blots) or measuring mRNA expression levels for the gene encoding the receptors. These three metrics can often be dissimilar. Reasons for the differences are often technical (such as selectivity of the antibodies or the receptor ligands, or adequacy of the mRNA sequence, or the much greater sensitivity of qPCR versus Western blots), but there are also good biological reasons for the discrepancies including receptor internalization

(which would be predicted to decrease ligand binding but not protein levels) or the many post-transcriptional events that regulate protein levels and/or function. A recent study examining a very large number of proteins found that the levels of transcripts and proteins only had a correlation coefficient of 0.27 (Ghazalpour et al., 2011). We previously examined this issue comparing D3R phMRI with ligand binding and mRNA expression levels (Choi et al., 2010). The phMRI results agreed better with the mRNA expression levels than they did with the ligand binding. Interestingly, in the Ghazalpour paper, they found much stronger association between transcript levels and clinical traits than with the protein levels (Ghazalpour et al., 2011). In this study, we found that there was very good qualitative concordance between the mRNA levels and Western blots - i.e. which receptors were altered in each brain region and their sign changes as to an increase or decrease. In addition, we found a good correlation between mRNA and protein levels ($R = 0.83$), but rather poor quantitative concordance in terms of the fold changes pointing out the limitations of Western blots for quantification of protein levels without using more elaborate techniques such as dilution series (Taylor et al., 2013).

Similar to a number of other studies of psychostimulants, we found an overall pattern of increased D1 and D3Rs in the METH animals as well as decreased D2R as measured by both protein levels or mRNA expression except in mPFCx where there was an increase in D2R (protein and mRNA). It should be stated, however, that in spite of years of study there are still discrepancies in the literature that are confounding enough that they raise questions about the techniques used. For instance, studies of non-human primates have found that cocaine administration can decrease D2 availability and that environment can have a profound effect on D2 availability (Nader, 2002), though not all studies are consistent in finding decreased D2R binding (reviewed in (Gould et al., 2014)). One study in humans that examined protein levels rather than receptor binding found a large increase in D1R in accumbens in methamphetamine addicts, but only a non-significant trend towards a decrease in D2R (Worsley et al., 2000). Studies in humans have found increased D3R (Staley and Mash, 1996) or no change (Meador-Woodruff et al., 1995). In vivo human studies of D3R using the PET ligand [11C]-(+)-PHNO in psychostimulant abusers shows increased D3 in globus pallidus and substantia nigra (reviewed in (Boileau et al., 2015)), though these studies, like those here, can be confounded by the fact that the B_{max} for D2R is much higher than for D3R (except in accumbens) and since D2 goes down and D3 goes up the mixed selectivity for D2/D3R for most ligands can confound the in vivo studies (see a discussion of this issue in (Choi et al., 2010) and Jenkins, 2012)).

In cocaine self-administering rats one study found that D3R binding increased only after 32 days of abstinence (Neisewander et al., 2004), whereas another study found a persistent increase after a single dose of cocaine (Le Foll et al., 2005). Two studies examining using either i.p. injections or self-administration of meth in rats found no changes in D1 or D2 receptor binding at any time point (Stefanski et al., 2002; Suzuki et al., 1997). Another study examining mRNA expression in animals administered i.p. meth found increased D1 mRNA in CPu but not accumbens (Ujike et al., 1991).

It would appear from a careful reading of the literature that increases in DA receptor binding seem to have less sensitivity to the changes in DAR compared to mRNA, protein levels or

now, phMRI. This may have to do with alterations in basal DA levels or synthesis rates. London's group has published papers showing a very small change in D2R binding (ca. 5%; (Kohno et al., 2016)) using PET of 18F-fallypride in methamphetamine addicts, and correlations between gray matter density in striatum with D2R binding potential. They have also shown an inverse correlation between D2R binding potential in striatum and impulsivity. Unfortunately PET studies of raclopride or fallypride can't distinguish between D2 and D3R, and our molecular data clearly show them going in opposite directions in most brain regions. Further, PET D2 data can be further confounded by D2 receptor internalization. Therefore, our take is that D2R, while likely declining with chronic meth, is harder to measure *in vivo*.

We examined D2R (protein and mRNA expression, *not* receptor binding) in VTA, CPu, mPFCx and NAc and found it decreased in all regions except mPFCx. Given the inhibitory afferent from mPFCx into the NAc which occurs (Doherty and Gratton, 1999) in comparison to the disinhibition of the subiculum input to the NAc it is clear these two nodes of the circuit provide potentially differential input via D2Rs. This may be counterbalanced by the effects of D1 and D3 both of which increased in every region studied. Increases in D1R protein levels in nucleus accumbens have been noted in human meth addicts (Worsley et al., 2000), as well as in rodent studies of meth conditioning using ligand binding (Ujike et al., 1991). Even single doses of psychostimulants can alter long term potentiation (LTP) (Ungless et al., 2001). Especially relevant to the results here, was a study showing that chronic meth treatment led to decreased LTP in the hippocampal-prefrontal cortex pathway, and that this impairment was mediated by D1R and not D2R (Ishikawa et al., 2005). Our study showed that one of the strongest effects we observed was a change of sign from negative to positive following meth challenge (consistent with an increase in D1R) in the CA1 region of the hippocampus and a huge increase in diFC from the CA1 region of the hippocampus to limbic striatum and prefrontal cortex (see Fig. 5).

4.5 Relation of Dopamine Receptor Modulation to Hemodynamic Changes

Based upon our prior work, we know that D1/D5R agonism leads to increased CBV and D2/D3R agonism leads to decreased CBV(Chen et al., 2005; Chen et al., 2010; Choi et al., 2006; Choi et al., 2010; Jenkins, 2012; Mandeville et al., 2013). Thus, increased D1R would be expected to lead to increased CBV and increased D2 and D3 would lead to decreased CBV, while decreased D2R expression would lead to increased CBV. The balance of these changes will, of course, be dependent upon the numbers of receptors assuming the affinities don't change, as well as the hemodynamic coupling constants (Jenkins, 2012). There is also some dependence upon both species and anesthetic. Halothane and isoflurane both increase CBF and decrease glucose metabolism globally in the brain, although the effects of isoflurane are far more profound than those of halothane (Maekawa et al., 1986) (Jenkins et al., 2005). Although halothane has been claimed to potentiate dopamine release, we examined the effect of halothane upon dopamine release induced by amphetamine and did not find a large difference between awake and anesthetized animals for dopamine release, however we compared awake and halothane-anesthetized primates and found a prolonged FWHM for the CBV induced by cocaine in the halothane-anesthetized animals (Mandeville et al., 2014). Therefore, there may be some effects of halothane upon the dopaminergic

effects, although these may be similar in the SAL and METH animals. Awake animals present other challenges such as learned helplessness and stimulation of auditory pain in the scanners.

The most striking change is the overall increase in CBV in METH*late* animals noted in many different brain regions. Given that D1R went up and D2R went down in most brain regions this pattern of increased CBV fits well with the observed receptor changes (both protein levels and mRNA expression levels). As mentioned above, there was a significant correlation between increases in D1 protein levels and increased fCBV ($R = 0.504$; $p < 0.05$) in the brain regions in which the latter was studied. We also examined the response to a D3 agonist. This drug induces an overall pattern of negative CBV changes that is most pronounced in the nucleus accumbens and the subiculum (Choi et al., 2010; Grundt et al., 2007). The METH animals show an increased negative response to the D3 agonist compared to the saline animals in the NAc and subiculum. If D3 is upregulated in these regions then one would predict a less positive CBV response in the accumbens and subiculum in response to methamphetamine challenge as noted. Unfortunately, 7-OHDPAT is not perfectly selective for D3/D2R – our results indicate that there is only about a two-fold increase in functional selectivity for D3/D2 in this dose range (Choi et al., 2010). Therefore, since there is also a decrease in D2 (and D2 can be predicted to have a higher Bmax in most brain regions) the D2 and D3 effects may well counterbalance each other when comparing challenges with either methamphetamine or with D2/D3 agonists. Unfortunately, there are no ligands that show high in vivo selectivity for D3 over D2 (or vice versa). The large increases in fCBV following meth challenge noted in multiple brain regions in the METH*late* animals is strongly suggestive of a large increase in D1R expression at this time point and, as discussed above, these are time points where D1R expression (protein and mRNA) showed much bigger changes in the METH*late* than METH*ear* animals. These results, as well as our extensive prior data, on the signs and magnitudes of CBV changes induced by various DAR ligands, suggest that phMRI provides a strong read-out on the relative changes in the DAR expression levels as a consequence of chronic meth administration.

Supplementary Material

Refer to Web version on PubMed Central for supplementary material.

Acknowledgments

Funding: Work partially supported by NIH/NIDA DA16187.

References

Adinoff B, Gu H, Merrick C, McHugh M, Jeon-Slaughter H, Lu H, Yang Y, Stein EA. Basal Hippocampal Activity and Its Functional Connectivity Predicts Cocaine Relapse. Biol Psychiatry. 2015

Andreoli M, Tessari M, Pilla M, Valerio E, Hagan JJ, Heidbreder CA. Selective antagonism at dopamine D3 receptors prevents nicotine-triggered relapse to nicotine-seeking behavior. Neuropsychopharmacology. 2003; 28:1272–1280. [PubMed: 12700694]

Black YD, Green-Jordan K, Eichenbaum HB, Kantak KM. Hippocampal memory system function and the regulation of cocaine self-administration behavior in rats. Behav Brain Res. 2004; 151:225–238. [PubMed: 15084439]

Blum K, Chen TJ, Downs BW, Bowirrat A, Waite RL, Braverman ER, Madigan M, Oscar-Berman M, DiNubile N, Stice E, Giordano J, Morse S, Gold M. Neurogenetics of dopaminergic receptor supersensitivity in activation of brain reward circuitry and relapse: proposing "deprivation-amplification relapse therapy" (DART). Postgrad Med. 2009; 121:176–196. [PubMed: 19940429]

Boileau I, Nakajima S, Payer D. Imaging the D3 dopamine receptor across behavioral and drug addictions: Positron emission tomography studies with [(11)C]-(+)-PHNO. Eur Neuropsychopharmacol. 2015; 25:1410–1420. [PubMed: 26141509]

Bossert JM, Adhikary S, St Laurent R, Marchant NJ, Wang HL, Morales M, Shaham Y. Role of projections from ventral subiculum to nucleus accumbens shell in context-induced reinstatement of heroin seeking in rats. Psychopharmacology (Berl). 2015

Brecht ML, Herbeck D. Time to relapse following treatment for methamphetamine use: a longterm perspective on patterns and predictors. Drug Alcohol Depend. 2014; 139:18–25. [PubMed: 24685563]

Caine SB, Thomsen M, Barrett AC, Collins GT, Grundt P, Newman AH, Butler P, Xu M. Cocaine self-administration in dopamine D(3) receptor knockout mice. Exp Clin Psychopharmacol. 2012; 20:352–363. [PubMed: 22867038]

Cervo L, Cocco A, Petrella C, Heidbreder CA. Selective antagonism at dopamine D3 receptors attenuates cocaine-seeking behaviour in the rat. Int J Neuropsychopharmacol. 2007; 10:167–181. [PubMed: 16426478]

Chen YC, Choi JK, Andersen SL, Rosen BR, Jenkins BG. Mapping dopamine D2/D3 receptor function using pharmacological magnetic resonance imaging. Psychopharmacology (Berl). 2005; 180:705–715. [PubMed: 15536545]

Chen YC, Galpern WR, Brownell AL, Matthews RT, Bogdanov M, Isacson O, Keltner JR, Beal MF, Rosen BR, Jenkins BG. Detection of dopaminergic neurotransmitter activity using pharmacologic MRI: correlation with PET, microdialysis, and behavioral data. Magn Reson Med. 1997; 38:389–398. [PubMed: 9339439]

Chen YC, Mandeville JB, Nguyen TV, Talele A, Cavagna F, Jenkins BG. Improved mapping of pharmacologically induced neuronal activation using the IRON technique with superparamagnetic blood pool agents. J Magn Reson Imaging. 2001; 14:517–524. [PubMed: 11747003]

Chen YI, Choi JK, Xu H, Ren J, Andersen SL, Jenkins BG. Pharmacologic neuroimaging of the ontogeny of dopamine receptor function. Dev Neurosci. 2010; 32:125–138. [PubMed: 20523024]

Chen YI, Famous K, Xu H, Choi JK, Mandeville JB, Schmidt HD, Pierce RC, Jenkins BG. Cocaine self-administration leads to alterations in temporal responses to cocaine challenge in limbic and motor circuitry. Eur J Neurosci. 2011; 34:800–815. [PubMed: 21896062]

Cho J, Sharp PE. Head direction, place, and movement correlates for cells in the rat retrosplenial cortex. Behav Neurosci. 2001; 115:3–25. [PubMed: 11256450]

Choi JK, Chen YI, Hamel E, Jenkins BG. Brain hemodynamic changes mediated by dopamine receptors: Role of the cerebral microvasculature in dopamine-mediated neurovascular coupling. Neuroimage. 2006; 30:700–712. [PubMed: 16459104]

Choi JK, Mandeville JB, Chen YI, Grundt P, Sarkar SK, Newman AH, Jenkins BG. Imaging brain regional and cortical laminar effects of selective D3 agonists and antagonists. Psychopharmacology (Berl). 2010; 212:59–72. [PubMed: 20628733]

Davidson C, Gopalan R, Ahn C, Chen Q, Mannelli P, Patkar AA, Weese GD, Lee TH, Ellinwood EH. Reduction in methamphetamine induced sensitization and reinstatement after combined pergolide plus ondansetron treatment during withdrawal. Eur J Pharmacol. 2007; 565:113–118. [PubMed: 17408614]

DiFeliceantonio AG, Mabrouk OS, Kennedy RT, Berridge KC. Enkephalin surges in dorsal neostriatum as a signal to eat. Curr Biol. 2012; 22:1918–1924. [PubMed: 23000149]

Doherty MD, Gratton A. Effects of medial prefrontal cortical injections of GABA receptor agonists and antagonists on the local and nucleus accumbens dopamine responses to stress. Synapse. 1999; 32:288–300. [PubMed: 10332804]

Friston KJ. Functional and effective connectivity: a review. Brain Connect. 2011; 1:13–36. [PubMed: 22432952]

Ghazalpour A, Bennett B, Petyuk VA, Orozco L, Hagopian R, Mungrue IN, Farber CR, Sinsheimer J, Kang HM, Furlotte N, Park CC, Wen PZ, Brewer H, Weitz K, Camp DG 2nd, Pan C, Yordanova R, Neuhaus I, Tilford C, Siemers N, Gargalovic P, Eskin E, Kirchgessner T, Smith DJ, Smith RD, Lusis AJ. Comparative analysis of proteome and transcriptome variation in mouse. PLoS Genet. 2011; 7:e1001393. [PubMed: 21695224]

Gilbert J, Newman AH, Gardner EL, Ashby CR Jr, Heidbreder CA, Pak AC, Peng XQ, Xi ZX. Acute administration of SB-277011A, NGB 2904, or BP 897 inhibits cocaine cue-induced reinstatement of drug-seeking behavior in rats: role of dopamine D3 receptors. Synapse. 2005; 57:17–28. [PubMed: 15858839]

Gould RW, Duke AN, Nader MA. PET studies in nonhuman primate models of cocaine abuse: translational research related to vulnerability and neuroadaptations. Neuropharmacology. 2014; 84:138–151. [PubMed: 23458573]

Grundt P, Prevatt KM, Cao J, Taylor M, Floresca CZ, Choi JK, Jenkins BG, Luedtke RR, Newman AH. Heterocyclic analogues of N-(4-(4-(2,3-dichlorophenyl)piperazin-1-yl)butyl)arylcarboxamides with functionalized linking chains as novel dopamine D3 receptor ligands: potential substance abuse therapeutic agents. J Med Chem. 2007; 50:4135–4146. [PubMed: 17672446]

Hall M, Eibe F, Holmes G, Bernhard P, Reutemann P, Witten IH. The WEKA data mining software: An update. SIGKDD Explorations. 2009; 11

Heidbreder CA, Gardner EL, Xi ZX, Thanos PK, Mugnaini M, Hagan JJ, Ashby CR Jr. The role of central dopamine D3 receptors in drug addiction: a review of pharmacological evidence. Brain Res Brain Res Rev. 2005; 49:77–105. [PubMed: 15960988]

Heidbreder CA, Thompson AC, Shippenberg TS. Role of extracellular dopamine in the initiation and long-term expression of behavioral sensitization to cocaine. J Pharmacol Exp Ther. 1996; 278:490–502. [PubMed: 8768696]

Henry DJ, White FJ. Repeated cocaine administration causes persistent enhancement of D1 dopamine receptor sensitivity within the rat nucleus accumbens. J Pharmacol Exp Ther. 1991; 258:882–890. [PubMed: 1890623]

Higley AE, Spiller K, Grundt P, Newman AH, Kiefer SW, Xi ZX, Gardner EL. PG01037, a novel dopamine D3 receptor antagonist, inhibits the effects of methamphetamine in rats. J Psychopharmacol. 2011; 25:263–273. [PubMed: 20142301]

Holstege, G. The basic somatic and emotional components of the motor system in mammals. In: Paxinos, G., editor. The Rat Nervous System. Academic Press; San Diego, CA: 1995. p. 244-252.

Ishikawa A, Kadota T, Kadota K, Matsumura H, Nakamura S. Essential role of D1 but not D2 receptors in methamphetamine-induced impairment of long-term potentiation in hippocampalprefrontal cortex pathway. Eur J Neurosci. 2005; 22:1713–1719. [PubMed: 16197511]

Jenkins BG. Pharmacologic magnetic resonance imaging (phMRI): imaging drug action in the brain. Neuroimage. 2012; 62:1072–1085. [PubMed: 22495143]

Jenkins, BG., Choi, JK., Mandeville, JB., Chen, Y. Brain fMRI in Pre-Clinical Pharmacological Stimulation Studies. In: Beckmann, N., editor. Pharmacology and Toxicology: Basic and Clinical Aspects: In vivo MR Techniques in Drug Discovery and Development. Vol. Chap. 8. CRC Press; 2005.

Kalivas PW, Volkow ND. The neural basis of addiction: a pathology of motivation and choice. Am J Psychiatry. 2005; 162:1403–1413. [PubMed: 16055761]

Keralapurath MM, Clark JK, Hammond S, Wagner JJ. Cocaine- or stress-induced metaplasticity of LTP in the dorsal and ventral hippocampus. Hippocampus. 2014; 24:577–590. [PubMed: 24464838]

Kilkenny C, Browne WJ, Cuthill IC, Emerson M, Altman DG. Improving bioscience research reporting: the ARRIVE guidelines for reporting animal research. PLoS Biol. 2010; 8:e1000412. [PubMed: 20613859]

Kohno M, Morales AM, Ghahremani DG, Hellemann G, London ED. Risky decision making, prefrontal cortex, and mesocorticolimbic functional connectivity in methamphetamine dependence. JAMA Psychiatry. 2014; 71:812–820. [PubMed: 24850532]

Kohno M, Okita K, Morales AM, Robertson CL, Dean AC, Ghahremani DG, Sabb FW, Rawson RA, Mandelkern MA, Bilder RM, London ED. Midbrain functional connectivity and ventral striatal dopamine D2-type receptors: link to impulsivity in methamphetamine users. Mol Psychiatry. 2016; 21:1554–1560. [PubMed: 26830141]

Kononenko I, Simec E, Robnik-Sikonja M. Overcoming the myopia of inductive learning algorithms with RELIEFF. Applied Intelligence. 1997; 7:39–55.

Konova AB, Moeller SJ, Tomasi D, Volkow ND, Goldstein RZ. Effects of methylphenidate on resting-state functional connectivity of the mesocorticolimbic dopamine pathways in cocaine addiction. JAMA Psychiatry. 2013; 70:857–868. [PubMed: 23803700]

Koob GF, Volkow ND. Neurocircuitry of addiction. Neuropsychopharmacology. 2010; 35:217–238. [PubMed: 19710631]

Lasseter HC, Xie X, Ramirez DR, Fuchs RA. Sub-region specific contribution of the ventral hippocampus to drug context-induced reinstatement of cocaine-seeking behavior in rats. Neuroscience. 2010; 171:830–839. [PubMed: 20870011]

Le Foll B, Diaz J, Sokoloff P. A single cocaine exposure increases BDNF and D3 receptor expression: implications for drug-conditioning. Neuroreport. 2005; 16:175–178. [PubMed: 15671872]

Lisman JE, Grace AA. The hippocampal-VTA loop: controlling the entry of information into long-term memory. Neuron. 2005; 46:703–713. [PubMed: 15924857]

Liu HS, Chefer S, Lu H, Guillem K, Rea W, Kurup P, Yang Y, Peoples L, Stein EA. Dorsolateral caudate nucleus differentiates cocaine from natural reward-associated contextual cues. Proc Natl Acad Sci U S A. 2013; 110:4093–4098. [PubMed: 23431137]

London ED, Kohno M, Morales AM, Ballard ME. Chronic methamphetamine abuse and corticostriatal deficits revealed by neuroimaging. Brain Res. 2015; 1628:174–185. [PubMed: 25451127]

Lu H, Stein EA. Resting state functional connectivity: its physiological basis and application in neuropharmacology. Neuropharmacology. 2014; 84:79–89. [PubMed: 24012656]

Lu H, Zou Q, Chefer S, Ross TJ, Vaupel DB, Guillem K, Rea WP, Yang Y, Peoples LL, Stein EA. Abstinence from cocaine and sucrose self-administration reveals altered mesocorticolimbic circuit connectivity by resting state MRI. Brain Connect. 2014; 4:499–510. [PubMed: 24999822]

Maekawa T, Tommasino C, Shapiro HM, Keifer-Goodman J, Kohlenberger RW. Local cerebral blood flow and glucose utilization during isoflurane anesthesia in the rat. Anesthesiology. 1986; 65:144–151. [PubMed: 3740503]

Mandeville JB. IRON fMRI measurements of CBV and implications for BOLD signal. Neuroimage. 2012; 62:1000–1008. [PubMed: 22281669]

Mandeville JB, Jenkins BG, Chen YC, Choi JK, Kim YR, Belen D, Liu C, Kosofsky BE, Marota JJ. Exogenous contrast agent improves sensitivity of gradient-echo functional magnetic resonance imaging at 9.4 T. Magn Reson Med. 2004; 52:1272–1281. [PubMed: 15562489]

Mandeville JB, Jenkins BG, Kosofsky BE, Moskowitz MA, Rosen BR, Marota JJ. Regional sensitivity and coupling of BOLD and CBV changes during stimulation of rat brain. Magn Reson Med. 2001; 45:443–447. [PubMed: 11241702]

Mandeville JB, Liu CH, Vanduffel W, Marota JJ, Jenkins BG. Data collection and analysis strategies for phMRI. Neuropharmacology. 2014; 84:65–78. [PubMed: 24613447]

Mandeville JB, Sander CY, Jenkins BG, Hooker JM, Catana C, Vanduffel W, Alpert NM, Rosen BR, Normandin MD. A receptor-based model for dopamine-induced fMRI signal. Neuroimage. 2013; 75:46–57. [PubMed: 23466936]

McKetin R, Najman JM, Baker AL, Lubman DI, Dawe S, Ali R, Lee NK, Mattick RP, Mamun A. Evaluating the impact of community-based treatment options on methamphetamine use: findings from the Methamphetamine Treatment Evaluation Study (MATES). Addiction. 2012; 107:1998–2008. [PubMed: 22564065]

Meador-Woodruff JH, Little KY, Damask SP, Watson SJ. Effects of cocaine on D3 and D4 receptor expression in the human striatum. Biol Psychiatry. 1995; 38:263–266. [PubMed: 8547449]

Milekic MH, Brown SD, Castellini C, Alberini CM. Persistent disruption of an established morphine conditioned place preference. J Neurosci. 2006; 26:3010–3020. [PubMed: 16540579]

Nader MA, Daunais JB, Moore T, Nader SH, Moore RJ, Smith HR, Friedman DP, Porrino LJ. Effects of cocaine self-administration on striatal dopamine systems in rhesus monkeys: initial and chronic exposure. Neuropsychopharmacology. 2002; 27:35–46. [PubMed: 12062905]

Neisewander JL, Fuchs RA, Tran-Nguyen LT, Weber SM, Coffey GP, Joyce JN. Increases in dopamine D3 receptor binding in rats receiving a cocaine challenge at various time points after cocaine self-administration: implications for cocaine-seeking behavior. Neuropsychopharmacology. 2004; 29:1479–1487. [PubMed: 15100700]

Paxinos, G., Watson, C. The Rat Brain in Stereotaxic Coordinates Sixth Edition. Elsevier Science; 2006.

Pickens CL, Airavaara M, Theberge F, Fanous S, Hope BT, Shaham Y. Neurobiology of the incubation of drug craving. Trends Neurosci. 2011; 34:411–420. [PubMed: 21764143]

Ray S, Di X, Biswal BB. Effective Connectivity within the Mesocorticolimbic System during Resting-State in Cocaine Users. Front Hum Neurosci. 2016; 10:563. [PubMed: 27881959]

Riedel A, Hartig W, Seeger G, Gartner U, Brauer K, Arendt T. Principles of rat subcortical forebrain organization: a study using histological techniques and multiple fluorescence labeling. J Chem Neuroanat. 2002; 23:75–104. [PubMed: 11841914]

Robinson TE, Becker JB. Enduring changes in brain and behavior produced by chronic amphetamine administration: a review and evaluation of animal models of amphetamine psychosis. Brain Res. 1986; 396:157–198. [PubMed: 3527341]

Robinson TE, Berridge KC. The neural basis of drug craving: an incentive-sensitization theory of addiction. Brain Res Brain Res Rev. 1993; 18:247–291. [PubMed: 8401595]

Robinson TE, Berridge KC. Review. The incentive sensitization theory of addiction: some current issues. Philos Trans R Soc Lond B Biol Sci. 2008; 363:3137–3146. [PubMed: 18640920]

Rogers JL, See RE. Selective inactivation of the ventral hippocampus attenuates cue-induced and cocaine-primed reinstatement of drug-seeking in rats. Neurobiol Learn Mem. 2007; 87:688–692. [PubMed: 17337218]

Schmidt HD, Anderson SM, Famous KR, Kumaresan V, Pierce RC. Anatomy and pharmacology of cocaine priming-induced reinstatement of drug seeking. Eur J Pharmacol. 2005; 526:65–76. [PubMed: 16321382]

Schmidt HD, Famous KR, Pierce RC. The limbic circuitry underlying cocaine seeking encompasses the PPTg/LDT. Eur J Neurosci. 2009; 30:1358–1369. [PubMed: 19788581]

Schwarz AJ, Gozzi A, Bifone A. Community structure in networks of functional connectivity: resolving functional organization in the rat brain with pharmacological MRI. Neuroimage. 2009; 47:302–311. [PubMed: 19345737]

Schwarz AJ, Gozzi A, Reese T, Bifone A. In vivo mapping of functional connectivity in neurotransmitter systems using pharmacological MRI. Neuroimage. 2007; 34:1627–1636. [PubMed: 17188903]

Sokal RR. Distance as a Measure of Taxonomic Similarity. Systematic Zoology. 1961; 10:70–78.

Staley JK, Mash DC. Adaptive increase in D3 dopamine receptors in the brain reward circuits of human cocaine fatalities. J Neurosci. 1996; 16:6100–6106. [PubMed: 8815892]

Stefanski R, Lee SH, Yasar S, Cadet JL, Goldberg SR. Lack of persistent changes in the dopaminergic system of rats withdrawn from methamphetamine self-administration. Eur J Pharmacol. 2002; 439:59–68. [PubMed: 11937093]

Steketee JD, Kalivas PW. Drug wanting: behavioral sensitization and relapse to drug-seeking behavior. Pharmacol Rev. 2011; 63:348–365. [PubMed: 21490129]

Suzuki H, Shishido T, Watanabe Y, Abe H, Shiragata M, Honda K, Horikoshi R, Niwa S. Changes of behavior and monoamine metabolites in the rat brain after repeated methamphetamine administration: effects of duration of repeated administration. Prog Neuropsychopharmacol Biol Psychiatry. 1997; 21:359–369. [PubMed: 9061779]

Taylor SC, Berkelman T, Yadav G, Hammond M. A defined methodology for reliable quantification of Western blot data. Mol Biotechnol. 2013; 55:217–226. [PubMed: 23709336]

Thompson D, Martini L, Whistler JL. Altered ratio of D1 and D2 dopamine receptors in mouse striatum is associated with behavioral sensitization to cocaine. PLoS One. 2010; 5:e11038. [PubMed: 20543951]

Tomasi D, Volkow ND, Wang R, Carrillo JH, Maloney T, Alia-Klein N, Woicik PA, Telang F, Goldstein RZ. Disrupted functional connectivity with dopaminergic midbrain in cocaine abusers. PLoS One. 2010; 5:e10815. [PubMed: 20520835]

Ujike H, Akiyama K, Nishikawa H, Onoue T, Otsuki S. Lasting increase in D1 dopamine receptors in the lateral part of the substantia nigra pars reticulata after subchronic methamphetamine administration. Brain Res. 1991; 540:159–163. [PubMed: 1829015]

Ungless MA, Whistler JL, Malenka RC, Bonci A. Single cocaine exposure in vivo induces long-term potentiation in dopamine neurons. Nature. 2001; 411:583–587. [PubMed: 11385572]

Worsley JN, Moszczynska A, Falardeau P, Kalasinsky KS, Schmunk G, Guttman M, Furukawa Y, Ang L, Adams V, Reiber G, Anthony RA, Wickham D, Kish SJ. Dopamine D1 receptor protein is elevated in nucleus accumbens of human, chronic methamphetamine users. Mol Psychiatry. 2000; 5:664–672. [PubMed: 11126397]

Zapata A, Chefer VI, Ator R, Shippenberg TS, Rocha BA. Behavioural sensitization and enhanced dopamine response in the nucleus accumbens after intravenous cocaine self-administration in mice. Eur J Neurosci. 2003; 17:590–596. [PubMed: 12581176]

Zhu J, Chen Y, Zhao N, Cao G, Dang Y, Han W, Xu M, Chen T. Distinct roles of dopamine D3 receptors in modulating methamphetamine-induced behavioral sensitization and ultrastructural plasticity in the shell of the nucleus accumbens. J Neurosci Res. 2012; 90:895–904. [PubMed: 22420045]

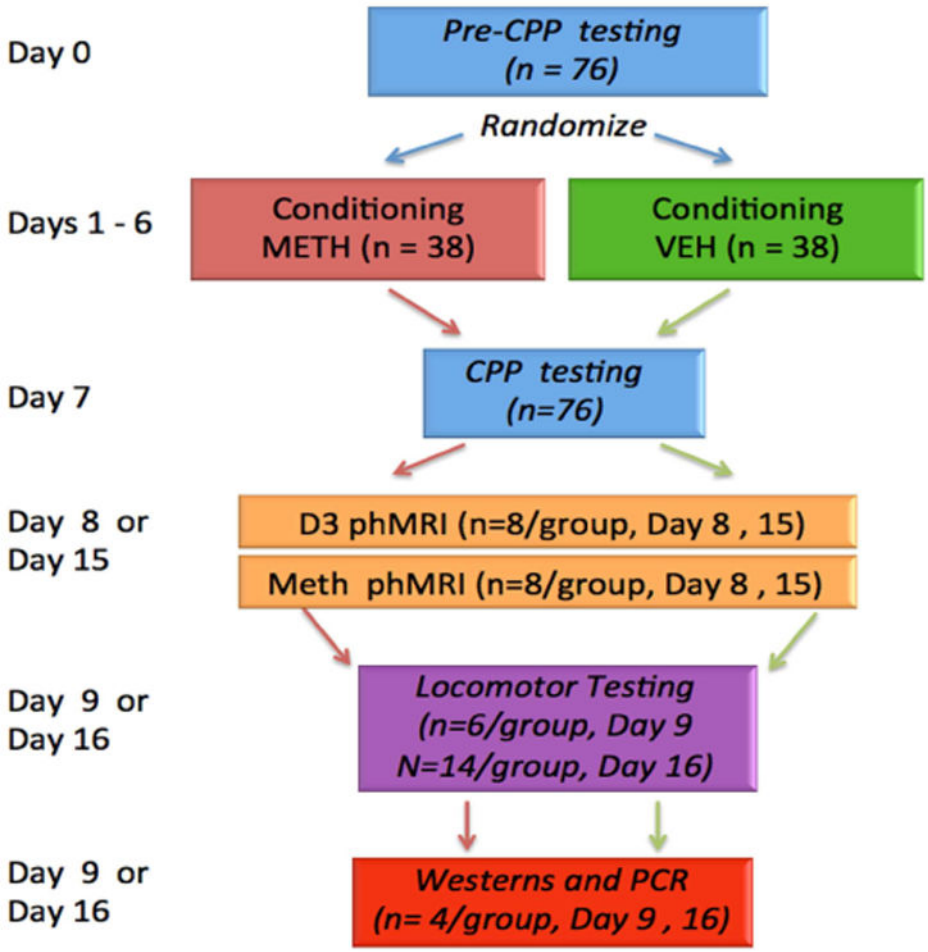

Figure 1.
Experimental design for the study. See Methods section for more detail about the individual components

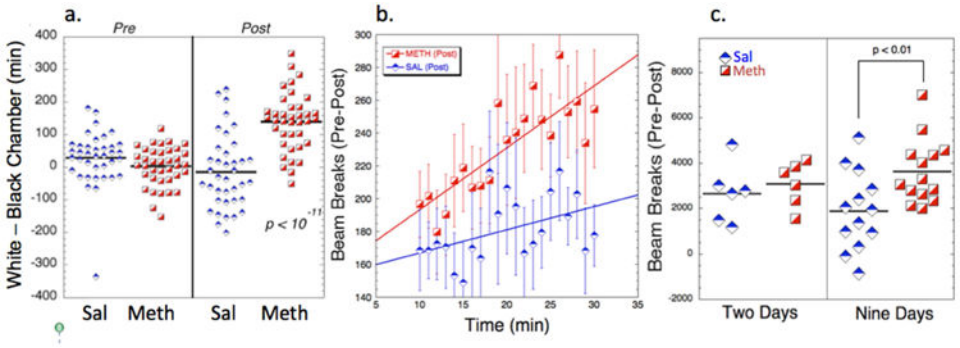

Figure 2.

Summary of behavioral data from all the animals studied. a) CPP data. The data are shown before and after conditioning with either meth or saline. There is a significant change in the Sal group after conditioning with saline where they prefer the black box (presumably showing aversion to the i.p. saline injection; $p < 0.02$ paired t-test). The METH group manifested a significant CPP ($p<10^{-11}$). There was a significant increase in the variance pre- and post-conditioning in both the SAL and METH animals as tested for using a Brown-Forsythe test for homogeneity of variances (SAL pre vs. post; $F^* = 10.08$; $p < 0.01$; METH pre vs. post; $F^* = 33.8$; $p < 0.001$). b) Locomotor testing of SAL and METH animals (post-pre) as a function of time following administration of 1 mg/kg i.p. meth. There is a significant difference between the METH and SAL animals (comparisons of the slopes showed $Z = 2.66$; $p<0.01$). c) comparisons of total beam breaks (post-pre) post-habituation of the locomotor testing showing a larger increase nine days after cessation of meth compared to two days ($p<0.01$; t-test).

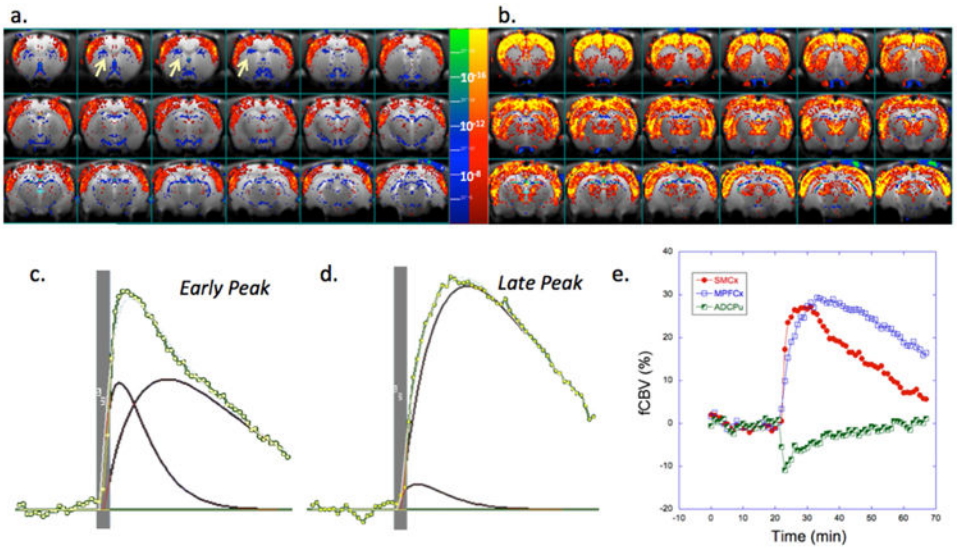

Figure 3.

Results of meth challenge (1mg/kg i.v.) in naïve animals (n=7). Shown is an average map of significant changes in fCBV. There are two general time courses observed including a shorter FWHM component with earlier time to peak mostly seen in cortical areas and a longer FWHM component with a longer time to peak mostly observed in subcortical areas (CPu, thalamus) but also in MPFCx. Maps are shown in a) and b) that derive from fits of the fCBV time course to a short (c) and long component (d). Yellow arrows indicate the anterior dorsal CPu (ADCPu). Shown in e) are the changes in CBV induced by the METH (injected at 20 min) in three regions of interest including sensorimotor cortex (SMCx), medial prefrontal cortex (MPFCx) and the anterior dorsal CPu (ADCPu; seen as negative CBV (blue) in panel a). The ADCPu has a negative fCBV change and short time course.

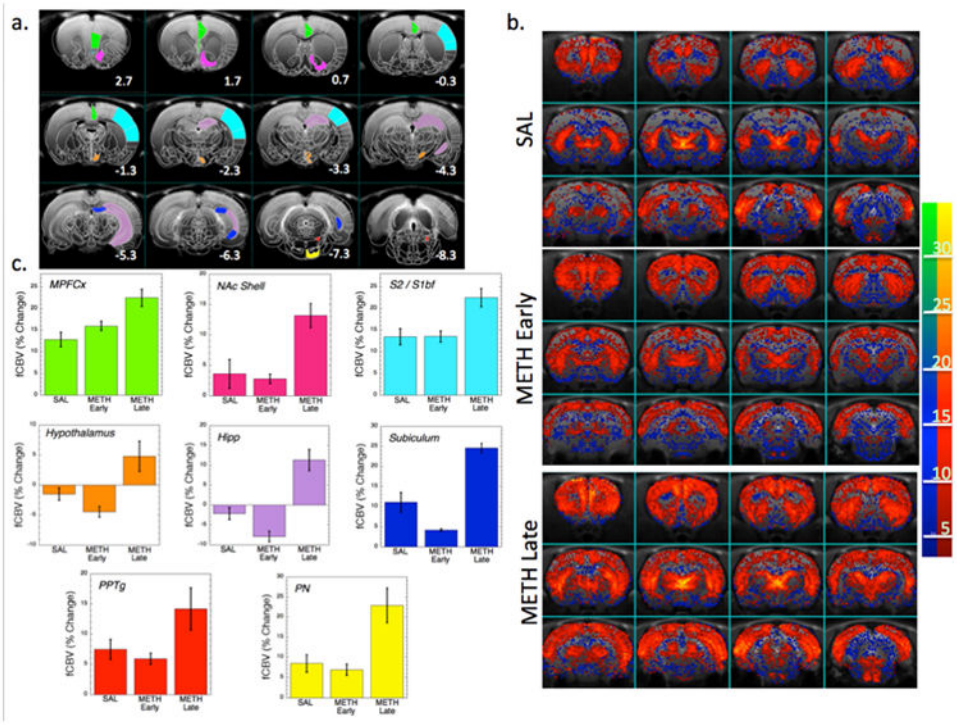

Figure 4.

Effects of methamphetamine challenge in METH and SAL animals. a) Template T2-weighted imaging overlaid with drawings from a Paxinos atlas showing a number of the important regions of interest including those identified as contributing the most to segregation between the groups. b). Parametric maps of the integrated fCBV change over 30 min following meth injection in the SAL, METH2 (METH early) and METH9 (METH late) groups. The METH late map is weighted towards more positive fCBV values. c) Bar graphs of the integrated fCBV change over 30 min in the regions identified as most important for group classification with colors corresponding to the ROIs indentified in a). MPFCx – medial prefrontal cortex, NAc Shell – nucleus accumbens shell, S2/S1BF – sensorimotor cortex including S1 and barrel field cortex, Hipp, hippocampus CA1 region, PPTg – pedunculopontine tegmental area, PN – pontine nucleus.

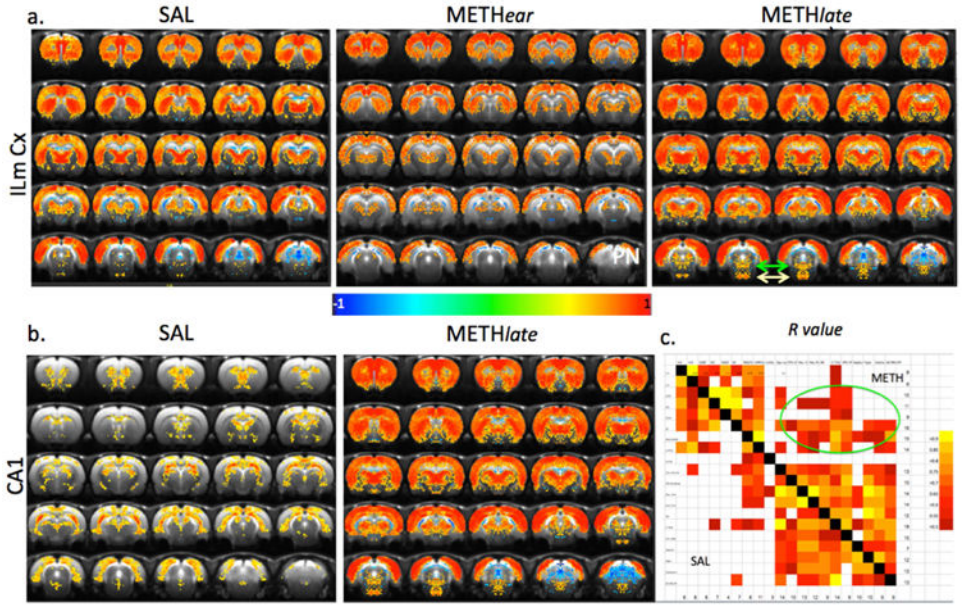

Figure 5.

Examples of altered connectivity following meth abstinence. a) Map of voxel-based diFC from infralimbic cortex in the SAL, METH*ear* and METH*late* groups. There is a decrease in many brain regions in the METH*ear* group and an increase in many brain regions including the sensorimotor cortices as well as the PPTg and pontine nucleus in the METH*late* group (the latter two structures are in the bottom of the images on the bottom row of a indicated with green arrows (PPTg) or yellow arrows (PN)). b) Map of voxel-based connectivity from CA1 region of hippocampus in the SAL and METH*late* groups. There is a strong connectivity between CA1 and CA3, septum, anterior dorsal CPu, ventral pallidum in the SAL group which completely alters in the METH*late* animals where there is strong connectivity to sensorimotor cortices, thalamus, accumbens, PN and PPTg. c) diFC matrix representing a random-effects model between various brain regions in the SAL and METH*late* animals. The circle shows increases in the METH*late* animals from limbic to sensorimotor regions. Empty squares were not statistically significant.

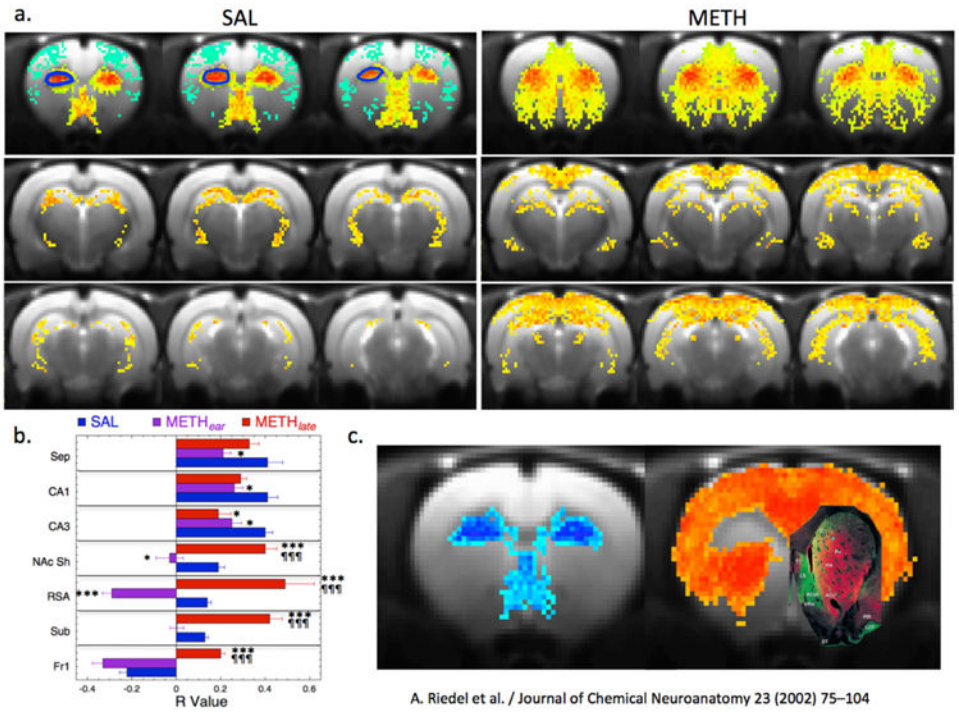

Figure 6.

Maps of functional connectivity from anterior dorsal CPu. a) Map of connectivity from ADCPu in the SAL and METH*late* group. There is negative connectivity to sensorimotor cortex and strong connectivity to septum, ventral pallidum, hypothalamus and hippocampus (CA1 and CA3) and lateral dorsal and posterior thalamus. Connectivity in the METH*late* animals shows decreased connectivity to CA1 and CA3, septum and hypothalamus and increased connectivity to NAc and subiculum. The outline in blue on the left side of the SAL map indicates the ROI used for the analyses reported in the fCBV data. b) Plot of alterations in connectivity induced by methamphetamine for the SAL, METHear and METHlate animals. * $p < 0.05$, or *** $p< 0.001$ for comparison to SAL animals. ¶¶¶ $p < 0.001$ for comparison to METH*ear* animals. c) Map of the negative and positive fCBV changes in the SAL group. Overlaid on the image is a map of calbindin binding in the striatum from Riedel et al. Journal of Chemical Neuroanatomy 23 (2002) 75–104. The areas of low binding are in green and the high areas are in red. These correspond very closely to the methamphetamine induced signs of the CBV changes (green areas showing negative fCBV changes and red areas that show positive fCBV values).

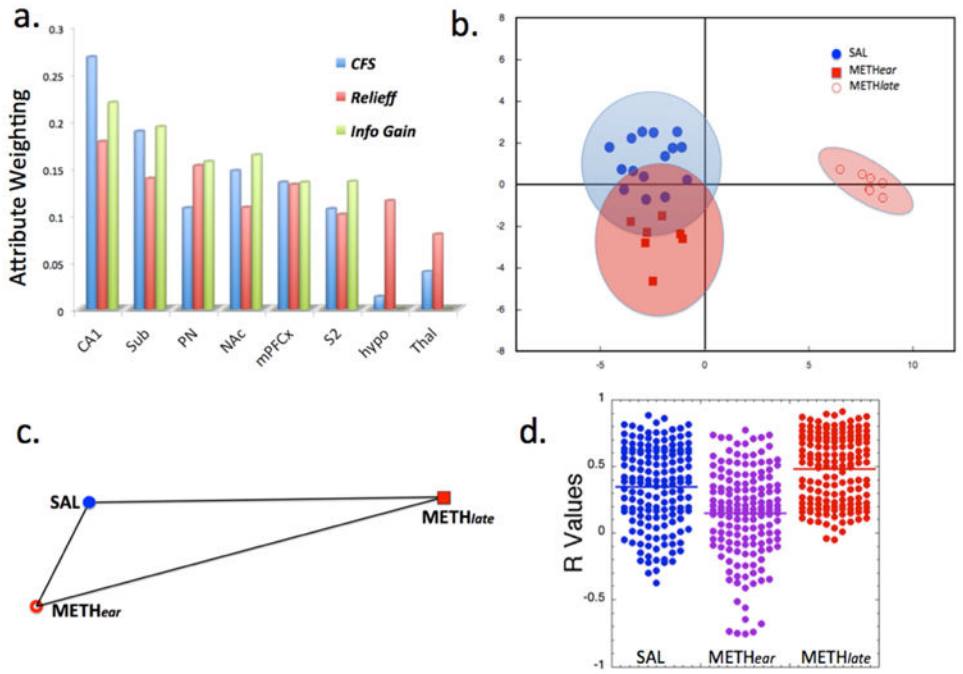

Figure 7.

Large separations between the METH*late* group and the SAL and METH*ear* groups, and relations between variables. a) Attribute selection for fCBV changes among 26 different brain regions using either Correlation feature selection (CFS), Relief-f or information gain algorithms showing the top 8 brain regions contributing to separation between the groups. b) Linear discriminant analysis based upon the fCBV data shows large separation between the METH*late* group and the SAL and METH*ear* groups. Wilk's lambda shows significant separation along the primary axis and not along the secondary (y) axis. The ellipses represent 95% confidence bounds for the groups. c) Relative Euclidean distances between the SAL, METH*ear* and METH*late* groups from the fCBV data. The METH*late* group is farthest from the other two groups. d) Distribution of R values determined from diFC from the brain regions shown in a) to the other brain regions for the three groups. It is clear that there is a decrease of overall connectivity in the METH*ear* group compared to the SAL ($p < 10^{-4}$) and that METH*late* is significantly greater than SAL ($p < 10^{-3}$) or METH*ear* ($p<10^{-4}$) (the p values listed are the maximum from using a t-test, Mann-Whitney U or Komolgorov-Smirnov test).

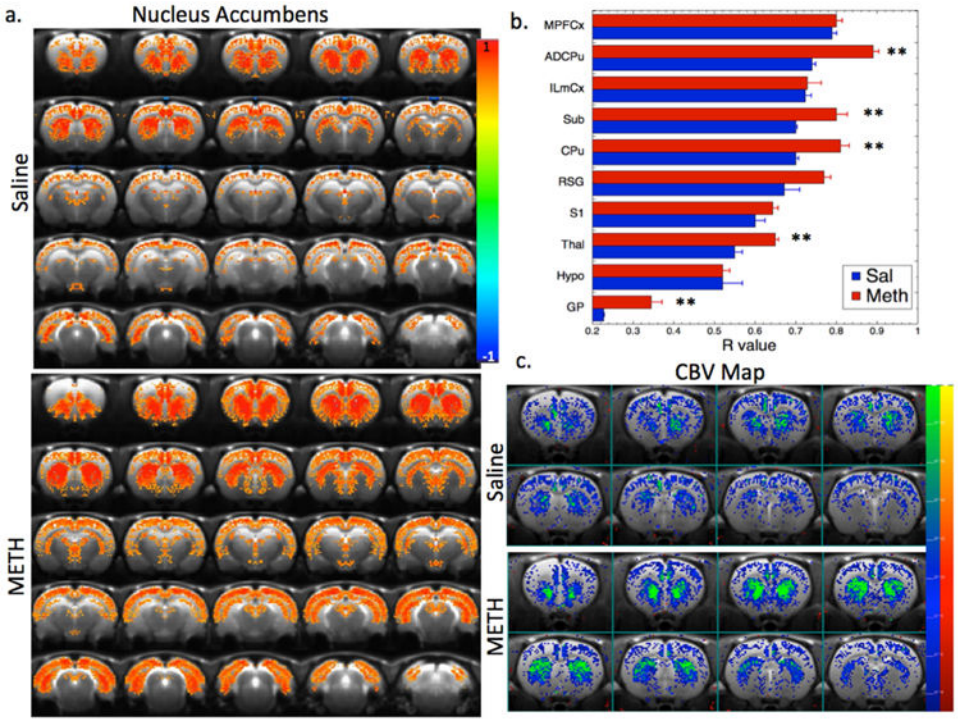

Figure 8.

Maps of changes in fCBV and diFC in response to a D3 preferring agonist. a) Maps of functional connectivity from a region in the nucleus accumbens in the SAL and METH*late* animals. There is a large increase in connectivity to a number of brain regions including ADCPu, subiculum (sub), CPu, globus pallidus (GP), and thalamus as seen in panel (b). c) Statistical parametric maps of changes in fCBV after challenge with the D3 selective agonist 7-OHDPAT in the SAL and METH animals (note the fCBV changes are negative following 7-OHDPAT). There is a large increase in the response (i.e. more negative fCBV change) in the NAc in the METH animals compared to SAL (see Table 2). ** $p < 0.01$ after correction for multiple comparisons using a Bonferroni-Holm test.

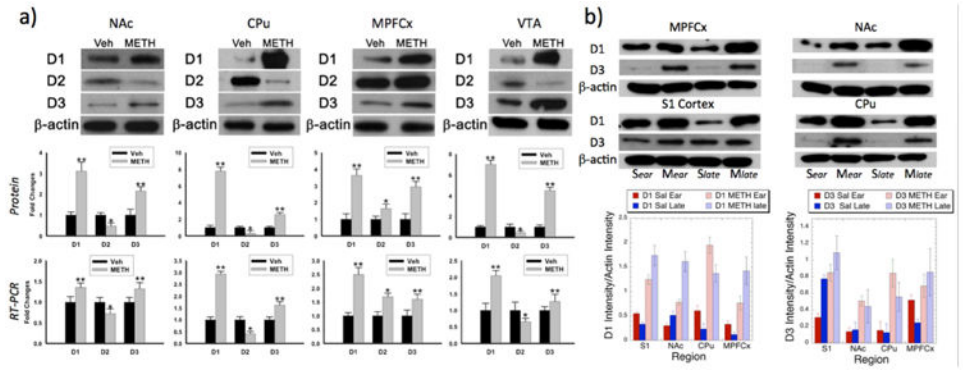

Figure 9.

Alterations in dopamine receptors as a function of methamphetamine treatment and time. a) Western blots in nucleus accumbens (NAc), caudate/putamen (CPu), medial prefrontal cortex (MPFCx) and ventral tegmental area (VTA) at 2 days of methamphetamine abstinence showing a generalized pattern of increases in D1 and D3 receptors and decreases in D2 receptors in the brain regions studied except in MPFCx where there was an increase in D2 receptors as well as D1 and D3. Quantitative results for the western blots are shown in the middle panel of a) showing changes in antibody binding to dopamine receptors of the METH treated animals relative to saline. In the bottom panel quantitative PCR data is shown for mRNA expression levels of the DAR showing identical patterns to those of the western blots including the decrease in D2 everywhere except MPFCx. b) These data show the effects of time on the DAR levels. The top panel shows blots taken from the same gel of animals at 2 days and 9 days after cessation of METH (M*ear*, M*late*) or saline (S*ear*, S*late*) in sensorimotor cortex (region S1), NAc, MPFCx and CPu. The bottom panel shows quantitative comparisons of either D1 or D3 optical density compared to β-actin in the gel. There were significant effects of treatment for D1 and D3 receptors in all brain regions and significant effects of time in NAc and CPu for D1R and significant effects of time for S1 for D3R. Each sample was composed of averages from four animals in each group and brain region. ** $p < 0.001$; * $p < 0.05$.

Table 1
Regional Changes in CBV Following METH Challenge

Brain Region	Saline (n=17)	Meth Early (n=8)	Meth Late (n=8)	P value
M1	11.80 ± 4.83	15.11 ± 3.87	17.26 ± 9.19	0.1330
M2	11.80 ± 3.91	15.40 ± 2.09	17.69 ± 8.92	0.0053
ILmCx	14.55 ± 4.89	20.81 ± 6.02	25.24 ± 11.38	0.0080
MPFCx	12.83 ± 3.51	15.97 ± 4.31	22.45 ± 8.05	0.0014 *
S2	13.44 ± 4.09	13.50 ± 4.47	22.49 ± 6.70	0.0011 *
S1BF	9.46 ± 3.85	9.71 ± 5.17	17.54 ± 8.71	0.0110
S1J	14.21 ± 5.98	14.27 ± 5.69	23.08 ± 10.85	0.0300
S1DZ	10.54 ± 4.27	10.36 ± 5.35	17.60 ± 9.48	0.0400
RS Cx	12.63 ± 5.24	14.23 ± 4.03	20.76 ± 10.60	0.0400
CPu	15.11 ± 4.56	15.49 ± 4.61	20.61 ± 6.11	0.0600
ADCPu	-6.01 ± 4.13	-5.27 ± 5.16	-1.05 ± 7.46	0.0860
NAc Core	7.17 ± 5.19	4.97 ± 2.63	14.52 ± 6.25	0.0030 *
NAc Shell	3.58 ± 4.89	2.76 ± 3.14	13.17 ± 8.09	0.0010 *
SN	-0.01 ± 3.79	-2.13 ± 4.41	5.64 ± 5.45	0.0066
C-Thal	14.57 ± 7.50	10.89 ± 4.54	24.04 ± 10.88	0.0110
VPL-VPM	2.62 ± 3.18	3.31 ± 3.18	8.04 ± 4.21	0.0060
Septum	0.93 ± 6.73	-1.04 ± 4.80	3.81 ± 6.45	0.3500
Hypothalamus	-1.51 ± 4.10	-4.44 ± 2.42	4.81 ± 6.70	0.0011 *
Subiculum	11.09 ± 10.21	4.14 ± 2.65	24.57 ± 9.72	0.0007 *
DG	-8.83 ± 5.51	-8.89 ± 3.00	-4.15 ± 6.69	0.4480
CA1	-2.17 ± 5.73	-7.93 ± 3.71	11.35 ± 7.61	0.0001 *
VTA	-2.43 ± 1.18	1.59 ± 5.80	2.73 ± 5.00	0.0400
PPTg	7.45 ± 6.21	5.88 ± 2.70	14.19 ± 9.92	0.0700
PN	8.43 ± 8.09	6.87 ± 3.86	22.93 ± 12.31	0.0001 *
SC	12.12 ± 7.00	10.29 ± 5.12	16.16 ± 7.37	0.2550
IC	11.30 ± 7.33	9.15 ± 4.46	14.53 ± 7.19	0.3500

Averaged changes in fCBV following challenge with 1mg/kg methamphetamine. M1 – motor cortex area 1, M2 – motor cortex area 2, ILmCx – infralimbic cortex, MPFCx – medial prefrontal cortex, S2 – sensorimotor cortex area 2, S1BF – sensorimotor cortex barrel field, S1J – sensorimotor cortex jaw area, S1DZ – sensorimotor cortex dysgranular region, RS Cx – retrosplenial cortex, CPu – caudate/putamen, AD-CPu – anterior dorsal CPu, NAc Core – nucleus accumbens core region, NAc Shell – nucleus accumbens shell region, SN – substantia nigra, C-Thal – central thalamus, VPL-VPM - ventral posterolateral and ventral posteromedial nuclei of the thalamus, DG – dentate gyrus of the hippocampus, CA1 – CA1 fields of hippocampus, VTA – ventral tegmental area, PPTg - pedunculopontine tegmental nucleus, PN – pontine nucleus, SC – superior colliculus, IC – inferior colliculus.

* Significant after correction for multiple comparisons using a Bonferroni-Holm.

Table 2
Regional Changes in CBV Following 7-OHDPAT Challenge

Brain Region (D3)	Saline (n=16)	METH Early (n=7)	METH Late (n=8)	P value
Nucleus Accumbens	-14.9 ± 4.5	-20.7 ± 3.7	-18.0 ± 5.2	0.01
ADCPu	-13.1 ± 4.2	-10.5 ± 2.1	-14.8 ± 5.1	0.16
CPu	-10.9 ± 3.2	-8.5 ± 2.1	-13.2 ± 4.3	0.03
Subiculum	-13.5 ± 5.5	-18.2 ± 3.7	-14.0 ± 5.3	0.10
ILmCx	-9.8 ± 5.8	-12.3 ± 3.8	-8.1 ± 4.2	0.27
MPFCx	-7.9 ± 4.4	-7.7 ± 2.6	-7.7 ± 4.8	0.99
Hypothalamus	-10.5 ± 4.2	-12.2 ± 3.2	-9.2 ± 4.3	0.38
Thalamus	-6.2 ± 5.4	-5.9 ± 1.5	-11.6 ± 6.2	0.04
S1 (layers III& IV)	-7.7 ± 4.0	-6.3 ± 1.6	-7.6 ± 3.2	0.81
IP	-14.0 ± 6.6	-13.4 ± 7.1	-14.0 ± 7.5	0.98

Averaged changes in fCBV following challenge with 0.2mg/kg 7-OHDPAT. ADCPu – anterior dorsal caudate/putamen, ILmCx – infralimbic cortex, MPFCx – medial prefrontal cortex, S1 – sensorimotor cortex area 1, IP – interpeduncular nucleus Critical p threshold was 0.006 for comparison of these regions Significant after correction for multiple comparisons.